

Report No. 350
November 2012

Office of Naval Research

Point of Contact: Dr. Patrick Purtell
Ship Hydrodynamics
U.S. Office of Naval Research
Code 331
875 N. Randolph St. Suite 1425
Arlington, VA 22203-1995
Tel: (703) 696-4308
Email: patrick.purtell@navy.mil

Final Report

Optimum Vessel Performance in Evolving Nonlinear Wave Fields

Department of Naval Architecture and Marine Engineering
University of Michigan
2600 Draper Drive
Ann Arbor, Michigan 48109-2145

Principal Investigator and Contact Person: Robert F. Beck
Tel: 734-764-0282
Fax: 734-936-8820
Email: rbeck@umich.edu

Administrative/Business Contact Person: Kathryn Dewitt
Office of Research
and Sponsored Projects
Tel: 734-763-6438
Email: dewitt@umich.edu

20121218064

Executive Summary

The MURI entitled "Optimum Vessel Performance in Evolving Nonlinear Wave Fields" ended on August 31, 2012. The total budget for the 5-year program was \$4,999,995.00. The research was conducted by a multi-disciplinary team of researchers from the University of Michigan (lead university), New Jersey Institute of Technology, Northwestern University, Ohio State University and the University of Washington. The researchers are experts in remote sensing/radar physics, nonlinear wave dynamics, ship dynamics, operations research and control theory. The MURI project supported 11 Ph.D. students along with several post docs, masters and undergraduate students. Project support was cited in a total of 35 Journal papers, 39 conference papers and 1 book chapter.

There were major accomplishments in all areas of the research. Major field trials of the radars were run in the Gulf of Alaska (2006), off the Northwest Coast of the US (2008), and off the pier at Army Field Research Facility in Duck, NC (2009). A unique time-domain algorithm was developed that allows real time processing of the coherent radar measurements of the sea surface velocities. Agreement between the radar predicted sea surface and sea truth measurements were good.

In order to project the radar measured sea surface forward in space and time, a pseudo-spectral wave model was developed that accounts for nonlinear wave-wave interactions up to arbitrary order, wave-current interactions, wave breaking, and wind-wave effects. Good agreement was shown between the numerical predictions and laboratory experiments at several different facilities around the world. To improve the wave field predictions, a variational technique was developed to assimilate radar measurements of the wave field every 2.5 seconds over an assigned assimilation period and forecast the future evolution of the wave field. Very good results were shown using actual radar data from the Alaska experiments.

Given the wave field, the ship motions can be determined by two different techniques that have been developed under the MURI program. The first is a nonlinear, time-domain, body-exact strip theory that runs in real time. Maneuvering in waves is simulated using a unique hydrodynamic axis system that follows the ship and couples the maneuvering and seakeeping responses through the nonlinear Euler equations of motion. The second is a three-dimensional, pseudo-spectral method in which the vessel can move along arbitrary paths through a random multidirectional wave field. The free surface evolution is efficiently evaluated with FFTs while the body boundary condition is time stepped using the Euler equations of motion. Integrals over the body surface are evaluated using a conventional flat panel method.

A dynamic programming model was developed that determines the optimal path through an evolving nonlinear wave field. The optimization integrates the detailed wave-field information collected by the radar with a seakeeping model that determines a path that minimizes the RMS vessel motion and incorporates a trade-off between travel time and reduced ship motions. Significant reductions in RMS roll motion were found by traveling the optimum path versus a straight line path with minimal increases in travel time. Various control algorithms were investigated to allow the ship to follow the optimum path with given constraints. In particular an adaptive model predictive control (MPC) strategy was explored to address the path following problem with varying operating environmental and model uncertainties.

The accomplishments achieved under this project have been wide ranging and of importance to the Navy. Much of the research has been directly transitioned over to the Navy FNC program entitled "Environmental and Ship Motion Forecasting (ESM F)." In addition, the computationally fast body-exact strip theory to predict the nonlinear responses of a ship to a seaway are being incorporated into version 3 of TEMPEST, the new, nonlinear, time-domain ship motion code being developed by the Navy.

Table of Contents

Executive Summary	i
List of Figures	iii
1.0 Project Overview	
1.1 Project Objective	1
1.2 Technical Approach and Sample Results	1
2.0 Technical Achievements	7
2.1 Radar System Simulation Model	7
2.2 Radar Measurements of Ocean Wave Fields	8
2.2.1 Non-Coherent/Coherent-on-Receive Marine Radars	8
2.2.2 Fully Coherent Radar	10
2.3 Nonlinear Wave Prediction	12
2.3.1 Pseudo-Spectral Wave Model Development and Validation	12
2.3.2 Radar Data Assimilation and Wave Forecasting	15
2.4 Ship Motion Prediction	17
2.4.1 Body-Exact Strip Theory	17
2.4.2 3-D Pseudo-Spectral Method	20
2.5 Real-Time Path Optimization and Vessel Control	23
2.5.1 Optimal Path Planning	23
2.5.2 Adaptive Vessel Control	24
3.0 Technology Transitions	27
4.0 Publications Acknowledging Support of the MURI	27
4.1 Ph.D. Dissertations Supported by the MURI	27
4.2 Book Chapters	27
4.3 Journal Articles	28
4.4 Conference Papers	30

List of Figures

Figure No.

1.1	Block diagram of the interrelations between the primary research areas of the MURI	1
1.2	FRF radar estimated surface elevations vs. wave gauge measured values.	2
1.3	Results of transient wave breaking tests at IOT.	3
1.4	Improvement in wave field predictions using assimilation.	3
1.5	ONR Tumblehome hull in forced heave motion in calm water.	4
1.6	S-175 turning circle in head waves.	5
1.7	Wave diffraction by a vertical, fixed cylinder, $ka = 1.0$.	5
1.8	Roll reduction for optimal path following.	6
2.1	Studies of shadowing effects on Doppler properties of low grazing angle backscatter.	7
2.2	An example of the radar simulator including NRCS, interferometric and Doppler retrievals.	8
2.3	Subset of wave field (left panel) estimated from conventional radar data set collected on April 8, 2006.	9
2.4	Subset of wave field (left panel) estimated from Doppler radar data set collected on August 13, 2008.	9
2.5	a) Directional wave spectra from cross sections. b) Directional wave spectra from Doppler shifts. c) Omnidirectional wave spectra from cross sections (black) and from the buoy (red).	11
2.6	Phase-resolved waves around the R/V Thompson obtained from CORAR's received Power (left) and Doppler offsets (right).	11
2.7	Comparison of various time series from CORAR and from the buoy on August 13, 2012.	12
2.8	Numerical simulations for resonant interaction between the peak wave numbers of wave fields characterized by the JONSWAP spectrum.	13
2.9	Laboratory experiments in an offshore engineering basin at the Institute of Offshore Technology in Canada.	13
2.10	Top panel: Two-dimensional wave breaking in a wave tank at the University of Michigan. Bottom left panel: Comparison of the total energy as a function of space. Bottom right panel: Comparison of surface elevations measured from three wave stations.	14
2.11	Surface elevation for the wave groups under wind condition $U_0 = 1.4\text{m/s}$.	14
2.12	Measured and predicted time histories of transient breaking wave.	16
2.13a	3-D view of simulated initial condition with 50% noise.	16
2.13b	3-D view of best-fit initial condition predicted by data assimilation scheme.	16
2.14	Calm water turning circle for S-175 container ship using Son and Nomoto (1981) models for the rudder, propeller and calm water resistance. $F_n = .15$, rudder angle = 35° .	19
2.15	S-175 turning circle and motion responses in beam seas.	20
2.16	3-D view of surface waves interacting with a cylinder, $ka = 1$.	21
2.17	Comparison of predicted pressure distribution on cylinder surface with Havelock's analytical solution, $ka = 1$.	21

2.18	Comparison of the response amplitude operators for a Series 60 ($C_B=0.6$) vessel in head seas ($U = 0$).	21
2.19	3-D panelization of R/V Thompson	22
2.20	Comparison of measured R/V Thompson motions with predictions from the 3D panel and RAO methods [West Coast Field Experiments (Aug 13, 2008,17:00 GMT)].	22
2.21	Roll reduction for optimal path following.	24
2.22	Simulation results of the ship response with the original (blue) and re-tuned (red) MPC path following controller in wave fields, green lines indicate the roll constraints.	25
2.23	Adaptive MPC schematic for ship path following.	26
2.24	A snapshot of integrated numerical test-bed.	26

1.0 PROJECT OVERVIEW

1.1. Project Objective

The overall objective of the MURI project was to develop the framework for an integrated system for the real-time control of maneuvering vessels in evolving nonlinear wave fields. The system would consist of: 1) a shipboard radar for real-time measurements of ocean wave fields; 2) a computationally efficient code to assimilate radar data and forecast the time-dependent evolution of nonlinear wave fields; 3) a numerical model to predict nonlinear ship motions in multidirectional wave fields in real time; and 4) control schemes and computationally fast algorithms to determine the optimum path of a vessel through a time-varying wave field based on specific vessel response constraints.

1.2. Technical Approach and Sample Results

The research conducted under this MURI has been divided into 4 different primary areas: real time radar wave field measurements; nonlinear wave prediction modeling and data assimilation; time-domain seakeeping/maneuvering models; and optimal routing and vessel control. Figure 1.1 describes the inter-relationship between the different areas and how they feed into an integrated system.

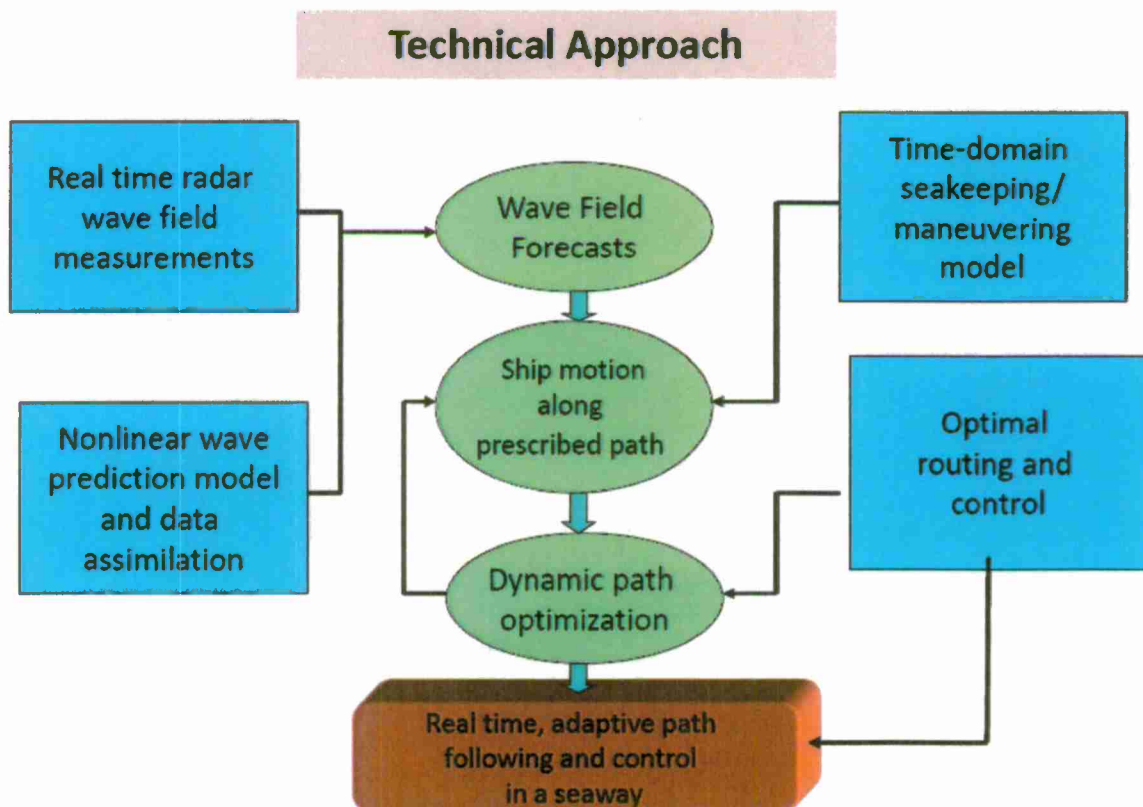


Figure 1.1. Block diagram of the interrelations between the primary research areas of the MURI.

Three major field experiments have been conducted as part of this MURI project to evaluate both coherent and non-coherent radar wave sensing technologies. The first experiment was conducted in the Gulf of Alaska in April of 2006 aboard the R/V Thompson out of the University of Washington. Three

wave buoys were deployed to gather sea truth and two radars were used to measure the waves. A follow up experiment, again aboard the R/V Thompson, was conducted in August of 2008 off the coast of Oregon with improved coherent radars. Good agreement was found with the buoy measurements for wave spectra and phase resolved waves. A third field experiment at the Army Field Research Facility in Duck, North Carolina was performed in November, 2009. The UofM radar was situated on the end of the pier and looked over the permanently mounted wave gauge array off the end of the pier. As seen in figure 1.2, the radar predicted wave time histories and the wave gauge measured values agreed well.

A significant amount of processing is required to determine the sea surface from the radar measurements. Under this project a unique time-domain algorithm was developed that allows real time processing of the coherent radar measurements of the sea surface velocities. All the calculations are made in the original range-azimuth (or polar) coordinates rather than transforming the data into rectangular coordinates. This allows the entire data set to be used, and corrections made for the look directional dependence of the measurements. Also developed was a radar system simulation tool that enabled more extensive studies of radar performance and to assess the influence of radar system properties on sea surface retrieval performance.

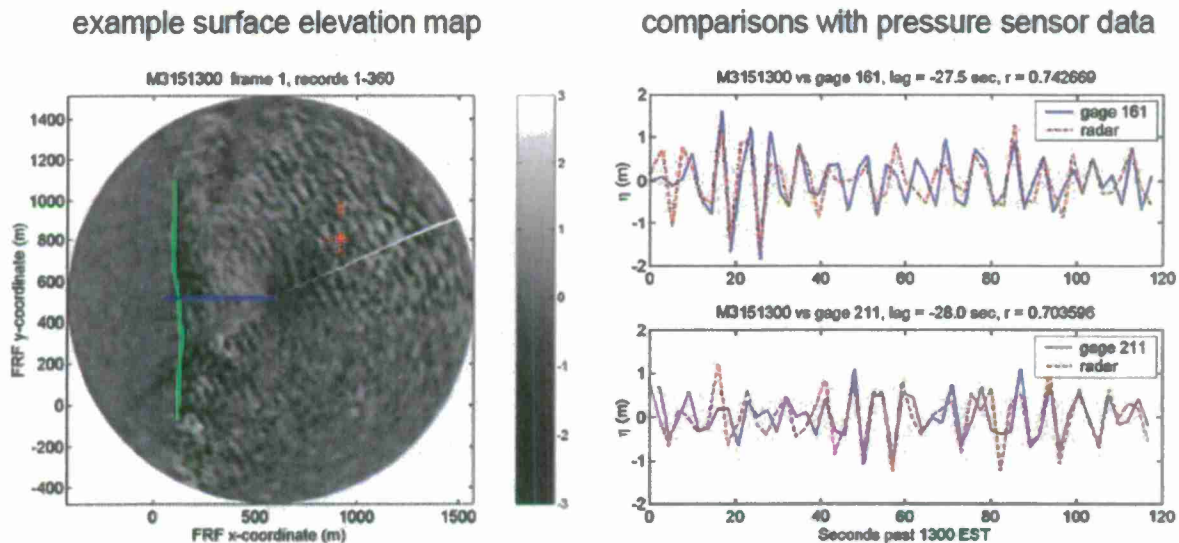


Figure 1.2. FRF radar estimated surface elevations vs. wave gauge measured values. The figure on the left shows the beach (green line), pier (blue line) and the wave gauge locations superimposed on the radar elevation map. The figure on the right is the comparison between the radar and wave gauge values.

In order to project forward in time the radar-measured sea surface, a pseudo-spectral wave model has been developed. The model accounts for nonlinear wave-wave interactions up to arbitrary order, wave-current interactions, wave breaking, and wind-wave effects. Several laboratory experiments were also conducted to verify the wave surface predictions and obtain data for the determination of empirical coefficients. Experiments have been conducted in the University of Michigan's wind-wave tank, the Institute for Ocean Technology (IOT) in Newfoundland, the Taiwan Hydraulics Laboratory and in the wave tank at Korean Advanced Institute for Science and Technology (KAIST), Daejeon, Korea. An example of the experimental results is shown in Figure 1.3. Note the good agreement between the numerical predictions of wave model and the experimental results even in post breaking waves.

A variational technique was developed to assimilate radar measurements of the wave field every 2.5 seconds and forecast the future evolution of the wave field. The scheme determines an "optimal" wave field that minimizes a cost function defined as the squared difference between the measure data and the

numerical prediction model over an assigned assimilation interval. Figure 1.4 shows the improvement in the wave field predictions using the assimilation procedure.

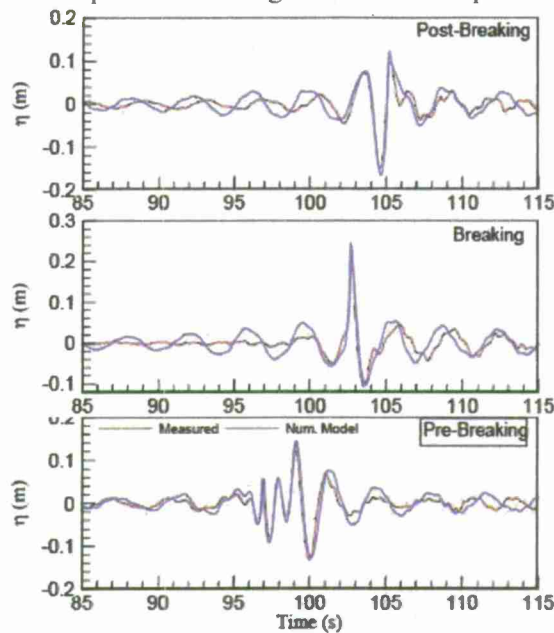


Figure 1.3. Results of transient wave breaking tests at IOT. The left frame is the wave elevation history at three different wave probes. The right frame shows the facility with 21 wave probes mounted on a horizontal truss.

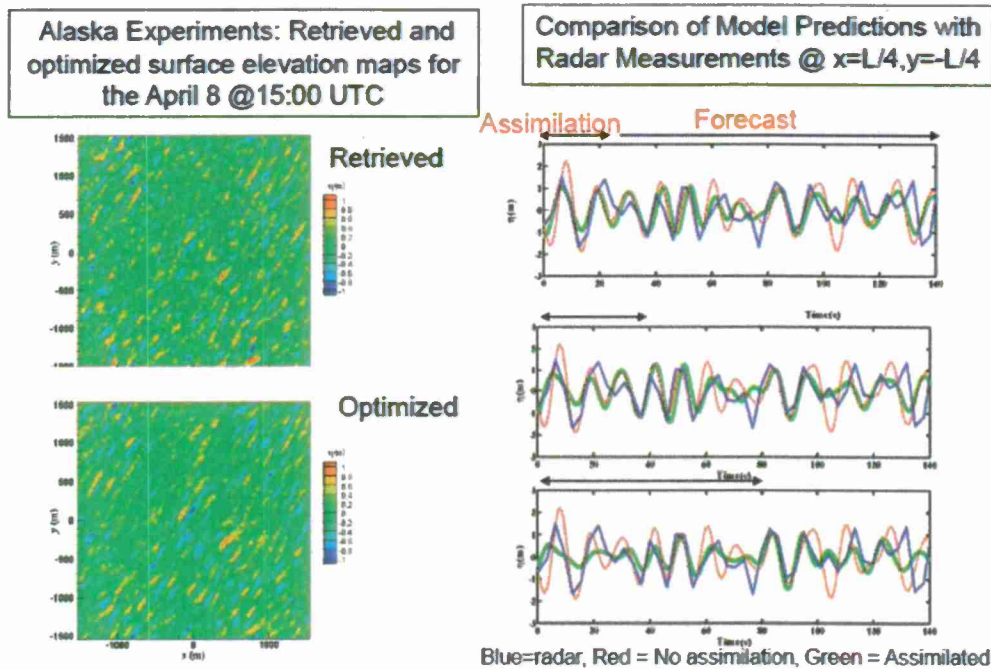


Figure 1.4. Improvement in wave field predictions using assimilation. Left panel shows the improvement for radar data from the Alaska experiments for the entire wave field. Right panel demonstrates the changes in the wave forecast for a specific point as the assimilation interval is lengthened.

Knowing the predicted wave field at the ship as a function of time, the ship motions can be predicted by a variety of methods. The ship motions computations have to be fast enough for real time path optimization and vessel control. Two different time-domain ship motion codes were developed as part of this MURI project. The first is a body-exact strip theory that runs in real time but has the limitations of strip theory. The body-exact strip theory makes the strip theory approximation in order to solve the hydrodynamic problem on two-dimensional strips along the vessel. On each strip, the exact hydrostatic and Froude-Krylov wave exciting forces are determined up to the instantaneous incident wave intersection with the body, but radiation and diffraction forces are determined using the linearized free surface condition and the body-exact body boundary condition. This allows the nonlinearities associated with the varying body shape to be properly accounted for while keeping computational time to a minimum. The viscous forces such as roll, sway and yaw damping are accounted for using empirical corrections. At the present time, the rudder and propeller forces are determined using traditional numerical models. Figure 1.5 shows comparisons with other theoretical linear and nonlinear methods to predict the heave force on the ONR tumble home hull due to forced heave. As can be seen, the linear results (LAMP 1 and LAMP 3) are pure sinusoids while the other results are highly nonlinear. The comparisons with other nonlinear methods are very good with a significant saving in computer time for UMBEST, the name of the code developed for this project. Figure 1.6 shows the path and ship motion predictions for the S-175 container ship in head seas and given a command to turn to starboard. Also shown are the results of model tests. The rudder and propeller model used in the code are simplified and probably explain the differences between the numerical and experimental results.

The second ship motion prediction technique being developed is a three-dimensional pseudo-spectral method. The body can move along arbitrary paths in a random multidirectional wave field. The free surface evolution is efficiently evaluated with FFTs while the body boundary condition is time stepped using the Euler equations of motion. Integrals over the body surface are evaluated using a conventional flat panel method. Figure 1.7 shows wave diffraction by a vertical, fixed cylinder and a comparison of the predicted pressure distribution with Havelock's analytic solution.

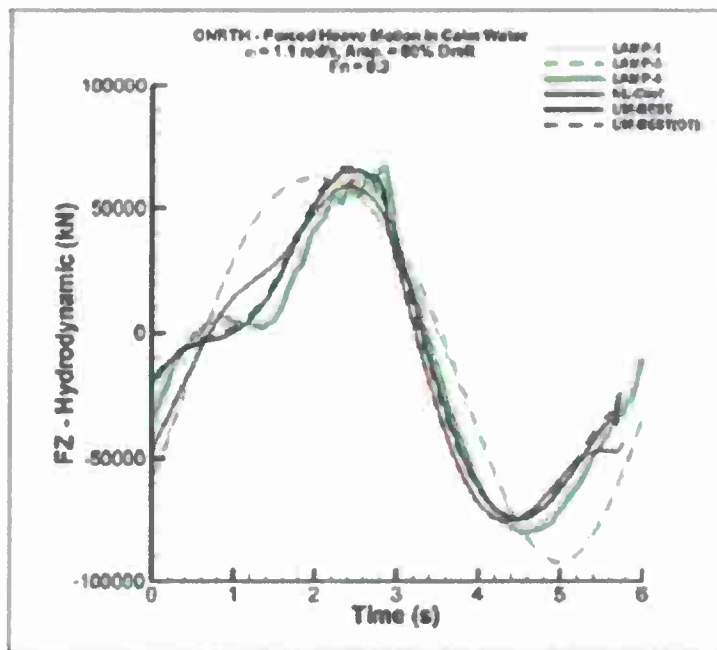


Figure 1.5. ONR Tumblehome hull in forced heave motion in calm water. Heave amplitude is 80% of the draft, Froude number = .3, oscillation frequency = 1.1 rad/sec model scale.

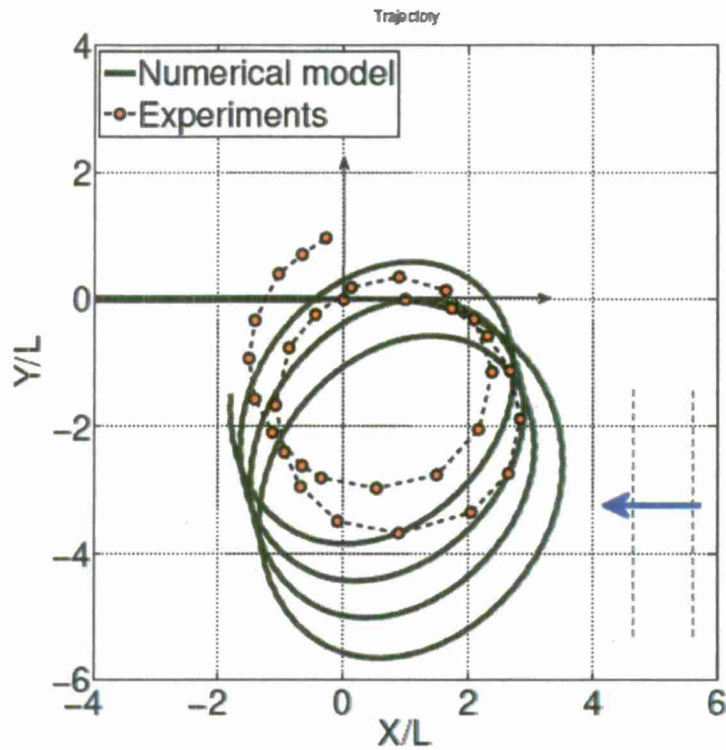


Figure 1.6. S-175 turning circle in head waves. Froude number = .15, rudder deflection is -35° , $H/\lambda = 1/60$, $\lambda/L = 1.2$.

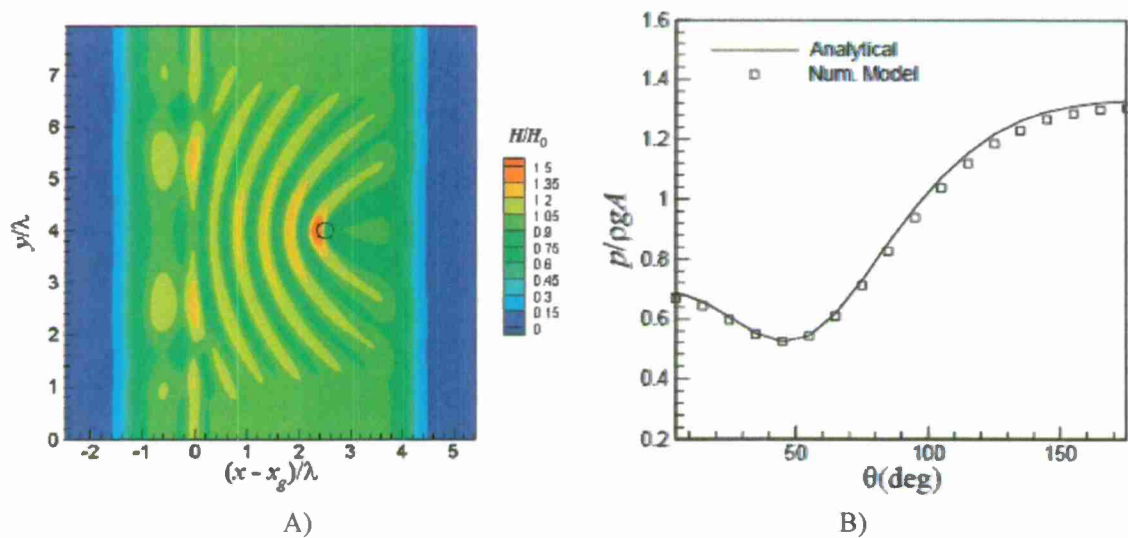


Figure 1.7. Wave diffraction by a vertical, fixed cylinder, $ka = 1.0$. A) is a view of the diffracted surface waves, B) Comparison of the predicted pressure distribution on the cylinder surface with Havelock's analytic solution.

A dynamic programming model was developed for the optimal routing and control that integrates the detailed wave-field information collected by the radar with a seakeeping model that determines a path that minimizes the RMS vessel motion and incorporates a trade-off between travel time and reduced ship motions. Various control algorithms were investigated to allow the ship to follow an optimum path with

given constraints. In particular an adaptive model predictive control (MPC) strategy was explored to address the path following problem with varying operating environmental and model uncertainties. Figure 1.8 shows the RMS roll reduction that is possible by following the curved path versus a straight line path between the start and the target way point. Since the sea state is random, the actual path and saving depends on the instant of starting.

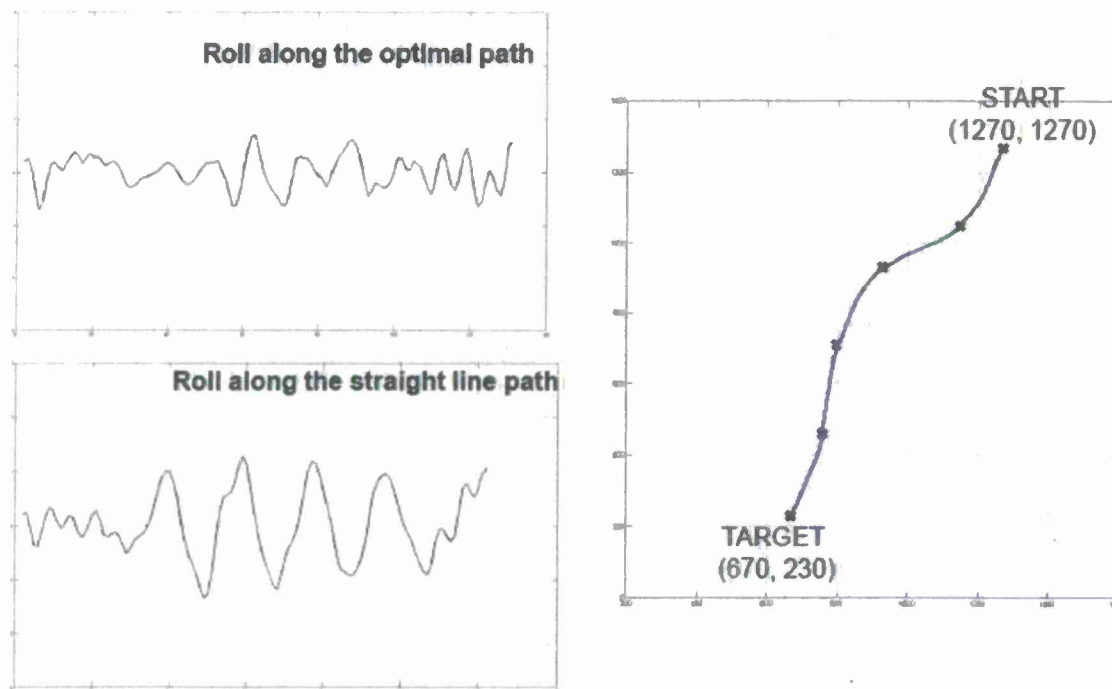


Figure 1.8. Roll reduction for optimal path following. S-175 in sea state 5 ($H_s = 3.25\text{m}$) and a ship speed of 10 m/s ($F_n = .24$) with a minimum turning radius of 300m. The RMS roll reduction along the optimal path was 108% and the additional travel time was 6%.

2. TECHNICAL ACHIEVEMENTS

The reports in this section were written by the technical lead in the given area of the research.

2.1 Radar System Simulation Model

Personnel: Joel Johnson, R.J. Burkholder, Chun-Sik Chae, Ninoslav Majurec, Ohio State University
David R. Lyzenga, University of Michigan

Detailed studies of the physics of low-grazing angle backscatter were conducted under the project in order to ensure that a robust understanding of radar observations was achieved to enable surface profile retrieval. Many insights were obtained through “numerically exact” simulations for one-dimensional sea surfaces conducted using the method of moments. These simulations included the prediction of range-resolved RCS, Doppler, and interferometric returns, so that profile retrievals with these three methods could be compared and contrasted. The results showed the relative advantages and disadvantages of each method, suggesting that retrievals that combine all three approaches may be advantageous in the future. The results also showed the ability of RCS and Doppler retrieval in particular to obtain some surface profile or velocity information even in shadowed regions of the surface. Figure 2.1 is an example of such information, in which Doppler spectra from a visible surface point (left) are contrasted with those from a shadowed surface point (right). Although measurable returns from shadowed regions occur only infrequently, when present the velocity information retrieved is consistent with the surface velocity despite the non-free space propagation experienced by such points.

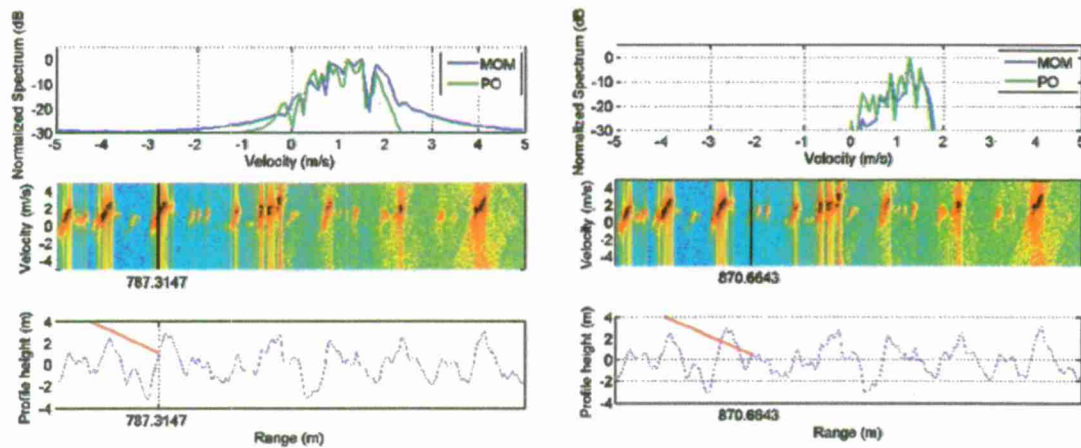


Figure 2.1 Studies of shadowing effects on Doppler properties of low grazing angle backscatter. Left plots consider a “visible” surface point, while right plots consider a shadowed point. Upper plots: Doppler spectra from “exact” method of moments (MOM) compared to approximate physical optics (PO) predictions at selected range location. Middle plots: Range-Doppler returns for all range locations of simulated profile; black line marks selected range location. Lower plots: Surface profile simulated; red “ray” marks selected range location corresponding to Doppler spectrum in upper plot.

Physical insights achieved by the numerical studies were incorporated into a simplified radar “system simulator” tool to enable more extensive studies of radar performance and to assess the influence of radar system properties on profile retrieval performance. The system simulation tool incorporates RCS, Doppler, and interferometric signal properties, and was also extended to consider imperfections such as local oscillator instabilities or the finite resolution of the radar analog-to-digital conversion. Figure 2.2

below presents an example of system simulator predictions; X-band (9.41 GHz) radar observation in a 20 MHz bandwidth is simulated for a sea surface corresponding to measurements performed in the “Alaska” field campaign of the MURI effort. Measurements of a 25 kW radar of antenna height 17 m operating at 24 rpm is simulated as the surface profile evolves. The system simulator models the “pulse-pair” radar measurements, including appropriate time-correlated speckle behaviors combined with thermal noise, so that errors in the pulse-pair retrieval can be captured. This simulation tool has transitioned to use in the “Environmental and Ship Motion Forecasting” program for sea-basing applications, and it is expected that transitions into other wavefield retrieval applications will occur in the future.

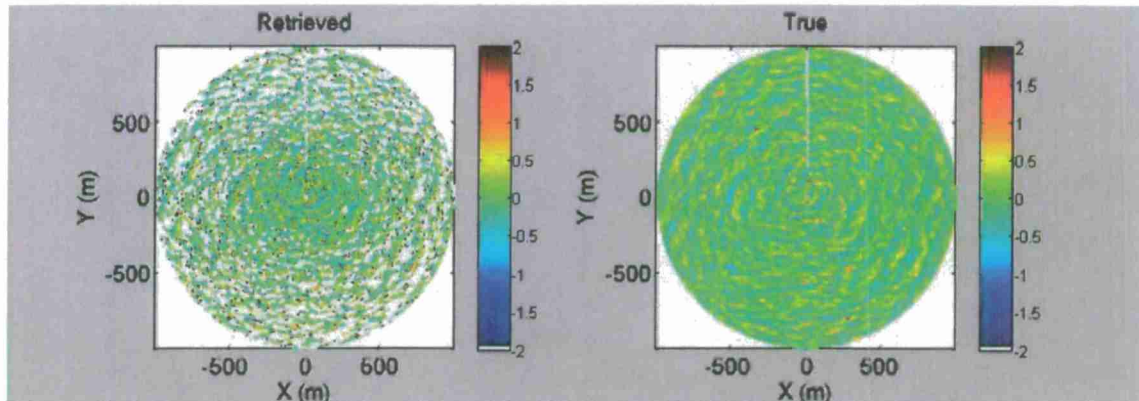


Figure 2.2 An example of the radar simulator including NRCS, interferometric, and Doppler retrievals

2.2 Radar Measurements of Ocean Wave Fields

2.2.1 Non-Coherent/Coherent-on-Receive Marine Radars

Personnel: David R. Lyzenga, University of Michigan

During the MURI project significant progress was made in the development of methods for measuring ocean wave fields using shipboard radar systems. Early in the project, in April 2006, a field experiment was carried out in the Gulf of Alaska in which data from the X-band and S-band navigational radars aboard the R/V Thompson was digitally recorded simultaneously with in situ measurements using several wave buoys. A theoretical model was derived relating the radar backscatter to the instantaneous surface elevation and slope, and this model was used to develop a processing algorithm for estimating the wave field from the radar data. One unique aspect of this algorithm was the fact that all calculations were made in the original range-azimuth or polar coordinates rather than transforming the data into rectangular coordinates. This allowed the entire data set to be used, and corrections to be made for the look directional dependence of the measurements, that is, for the fact that optimal measurements of a given wave component are obtained when the radar look direction is nearly parallel or anti-parallel to the wave propagation direction.

In August 2008, a second field experiment was carried out off the coast of Northern California using a Doppler radar developed for the University of Michigan by Imaging Science Research, Inc. under a DURIP project. The previously developed processing algorithm was extended to utilize the Doppler velocity data provided by this radar. This new algorithm makes use of the fact that the radial velocity can be considered as the derivative of the velocity potential function Φ in the range direction, and the surface elevation is proportional to the time derivative of this function (Nwogu and Lyzenga, 2010). Thus, the surface elevation can be retrieved in principle by integrating the Doppler velocity along each range line to estimate Φ and taking the time derivative of Φ by frame-to-frame differencing. Initially, these operations

were carried out by means of a spatial Polar Fourier transform algorithm developed during this project, and a Fast Fourier transform (FFT) in the time dimension. Later, a time-domain version of the algorithm was developed to replace the temporal FFT, paving the way for eventual real-time processing of the data. Some example results obtained by applying the time domain processing algorithm to data sets from both field experiments are shown in Figures 2.3 and 2.4.

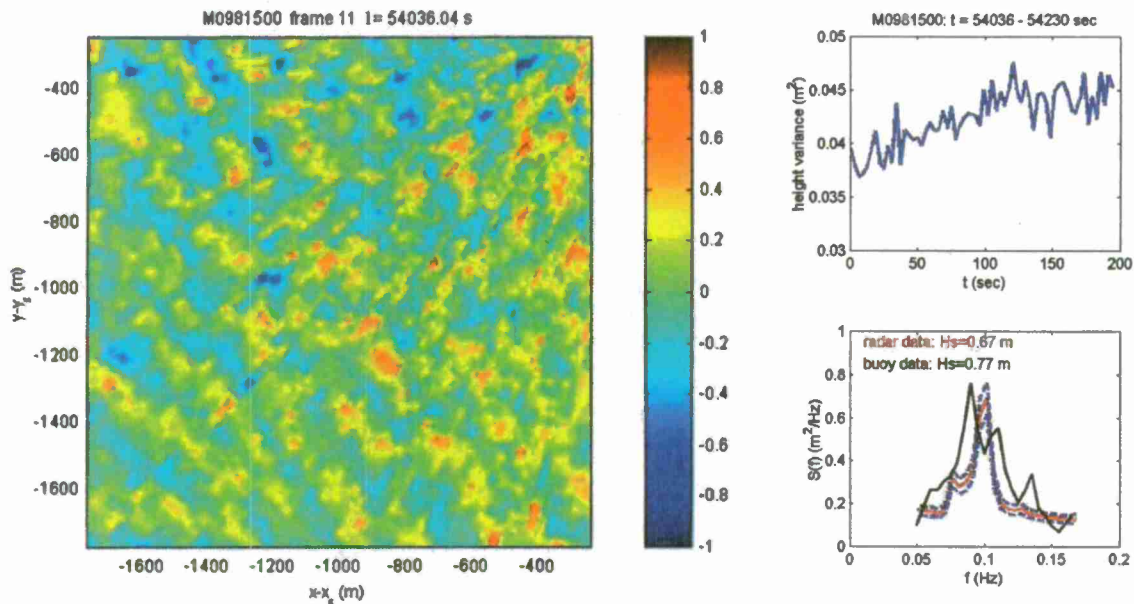


Figure 2.3. Subset of wave field (left panel) estimated from conventional radar data set collected on April 8, 2006. Upper right panel shows height variance over this region as a function of time, and lower right panel shows estimated frequency spectrum compared with buoy measurements.

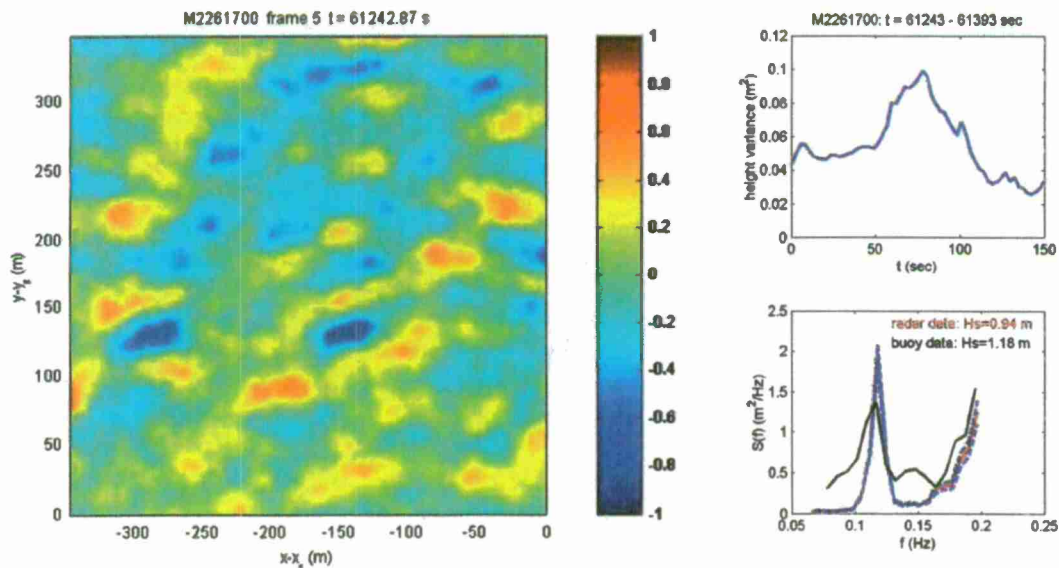


Figure 2.4. Subset of wave field (left panel) estimated from Doppler radar data set collected on August 13, 2008. Upper right panel shows height variance over this region as a function of time, and lower right panel shows estimated frequency spectrum compared with buoy measurements.

Reference

O.G. Nwogu and D.R. Lyzenga, (2010) "Surface-Wavefield Estimation From Coherent Marine Radars," *Geoscience and Remote Sensing Letters*, 7 (DOI:10.1109/LGRS.2010.2043712).

2.2.2 Fully Coherent Radar

Personnel: William J. Plant, Applied Physics Laboratory, University of Washington, Seattle, WA

This section summarizes the work carried out by the Applied Physics Laboratory of the University of Washington for the MURI. Additional details are provided in the paper entitled "Measurement of Winds, Waves, and Currents with a Shipboard Coherent Radar" by Plant et al. (2012).

In August 2008, we deployed a VV-polarized, X-band (9.36 GHz), coherent radar on a UNOLS ship, the R/V Thompson, on a cruise along the west coast of the United States. The purpose of the cruise was to measure phase-resolved waves around the ship using the low-grazing angle sea return to the radar. The radar signal also proved capable of determining winds and currents around the ship. In the paper we compare these measurements of winds, waves, and currents with similar quantities measured by more standard techniques. Wind speeds were determined from wind speed dependence of the upwind maximum of the mean normalized radar cross section (NRCS) measured by the radar. These wind speeds compared well with those measured by the shipboard anemometer. The 180° ambiguity of the wind direction from the radar (because upwind and downwind maxima were nearly the same) was overcome by looking at the direction of propagation of wind waves determined from the wave dispersion relation. This dispersion relation was derived from wave number-frequency spectra obtained from space-time images of both the NRCS and the Doppler offsets. Fitting the dispersion relation to the standard form including currents allowed the current magnitude and direction to be determined. The component of current in the direction of the ship heading agreed well with currents from the ship's pitot tube. Finally, phase-resolved wave fields around the ship were determined using wave-induced variations in the NRCS and Doppler offsets under the assumptions that our k-space azimuthal resolution was high, that Fourier components in each direction could be extended to the entire region around the ship, and that NRCS variations were mostly due to changes in local grazing angle, ie, tilt modulation. These phase-resolved wave heights compared fairly well with those measured by a buoy. Significant wave heights and mean omnidirectional spectra also agreed reasonably well with the buoy measurements. However, a close look at the spectra revealed that additional modulation transfer functions were probably necessary to produce accurate wave fields from NRCS variations.

In the following, Figure 2.5 shows comparisons of wave height variance spectra from the radar and from a buoy deployed near the ship. Figure 2.6 presents the two-dimensional phase-resolved wave fields around the ship derived from normalized radar cross sections (NRCS) and from Doppler shifts.

Figure 2.7 shows comparisons of time series of phase-resolved wave heights from the radar and from the buoy. Also shown are comparisons of these time series for wave heights from the radar determined from Doppler shifts and from the NRCS.

Our conclusion is that while none of the radar measurements agreed perfectly with those from more standard instruments, the agreement was sufficiently promising to encourage continued development of the radar techniques.

References

Plant, W.J., Chatham, G., Hayes, K., and Keller, W.C. (2012) "Measurement of Winds, Waves, and Currents with a Shipboard Coherent Radar," to be submitted to *Journal of Atmospheric and Oceanic Technology*.

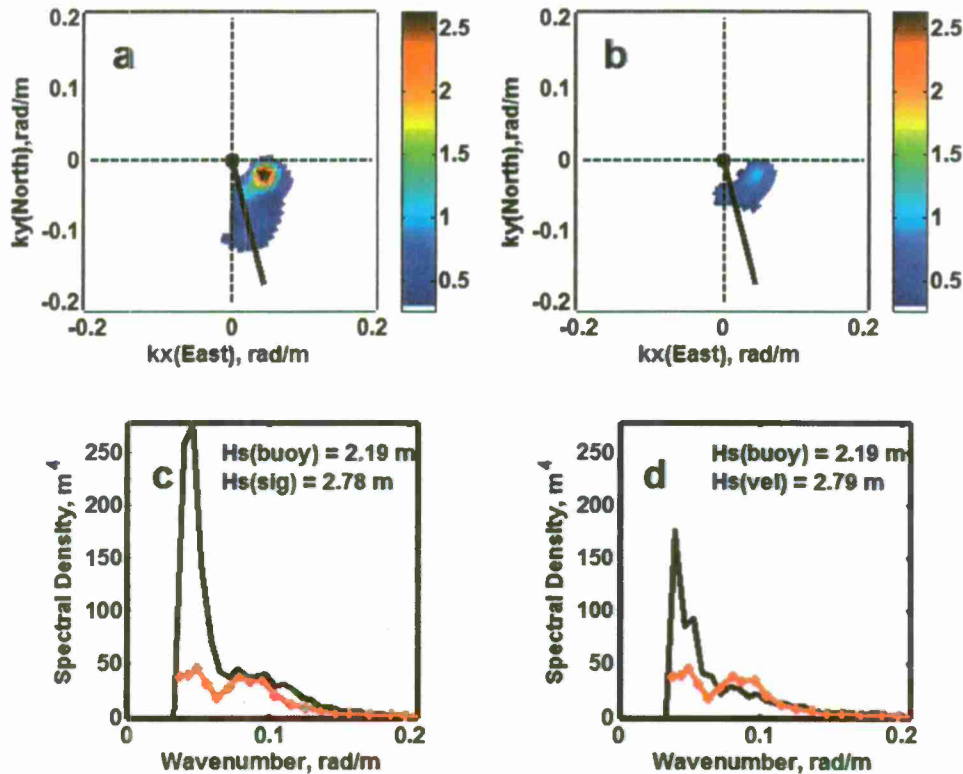


Figure 2.5. a) Directional wave spectra from cross sections. b) Directional wave spectra from Doppler shifts. c) Omnidirectional wave spectra from cross sections (black) and from the buoy (red). d) Omnidirectional wave spectra from Doppler shifts (black) and from the buoy (red). The black line in the upper panels show the direction toward which the wind blows, from the center out. Significant wave heights, H_s , are shown in the upper right corner of the lower panels. Data were taken on August 13, 2008 at 17:55 UTC.

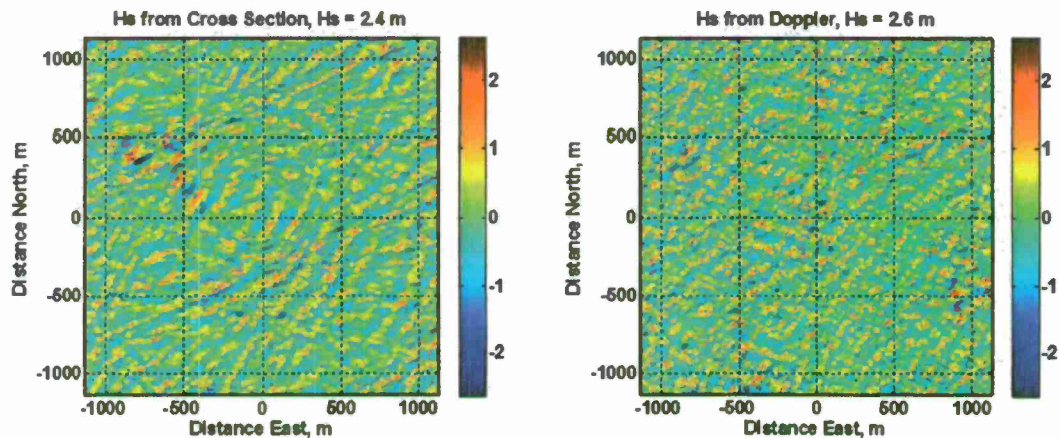


Figure 2.6. Phase-resolved waves around the R/V Thompson obtained from CORAR's received power (left) and Doppler offsets (right). Data were taken on August 13, 2008 at 17:55 UTC.

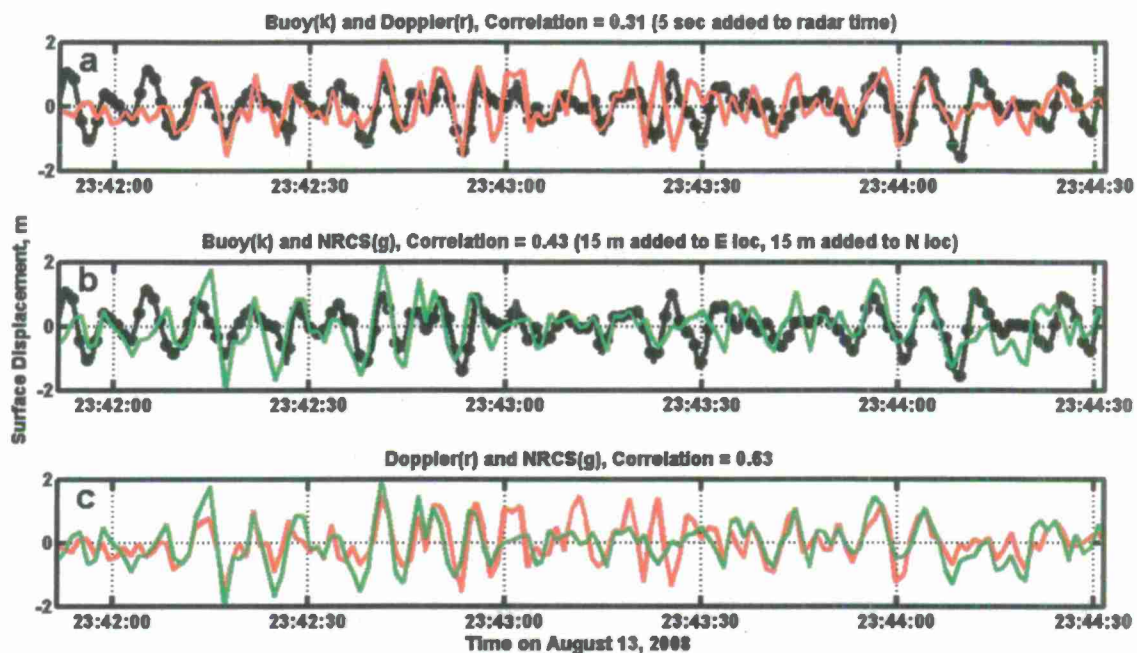


Figure 2.7. Comparison of various time series from CORAR and from the buoy on August 13, 2012. a) Comparison of buoy wave heights (black) and those from Doppler shifts (red). b) Comparison of buoy wave heights and those from cross sections (green). c) Comparison of wave heights from Doppler shifts (red) and from cross sections (green). The 5 second offset in the two upper comparisons allows for a small shift in the radar times.

2.3 Nonlinear Wave Prediction

2.3.1 Pseudo-Spectral Wave Model Development and Validation

Personnel: Wooyoung Choi, New Jersey Institute of Technology
 Marc Perlin, University of Michigan
 Zhigang Tian, Korea Advanced Institute of Science and Technology (KAIST)

The major accomplishments are:

- We have developed a parallel pseudo-spectral wave prediction model based on asymptotic expansion technique and have carried out extensive numerical simulations for a wide range of physical parameters.
- We have performed two sets of laboratory experiments for both breaking and non-breaking waves: (1) Three-dimensional wave tank experiments at the Institute of Ocean Technology in Canada for the evolution of short-crested waves; (2) Two-dimensional wave tank experiments at the University of Michigan for frequency-focusing breaking waves. These experiments have been used to validate the wave prediction model.

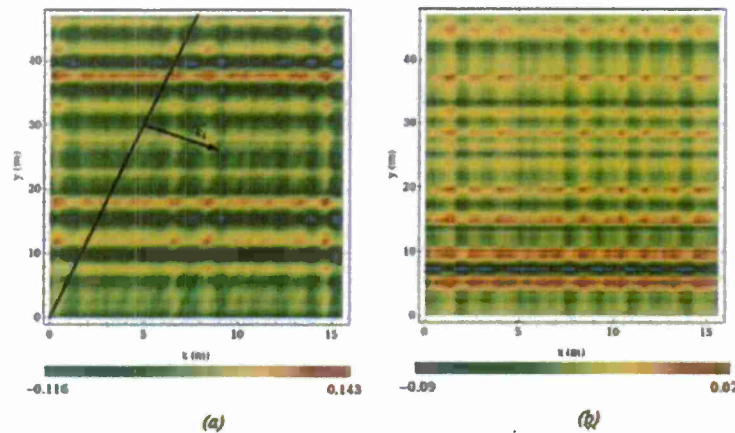


Figure 2.8. Numerical simulations for resonant interaction between the peak wave numbers of wave fields characterized by the JONSWAP spectrum: Density plots for the surface elevation at $t=50$ s, for a peak enhancement (a) $\gamma=20$ and (b) $\gamma=3.3$. For the case of $\gamma=20$, the resonant wave is clearly visible, while it is hardly noticeable for the case of $\gamma=3.3$.



Figure 2.9. Laboratory experiments in an offshore engineering basin at the Institute of Offshore Technology in Canada.

- We have developed the eddy viscosity model to predict the evolution of post-breaking waves with accurately describing energy dissipation due to wave breaking.
- We have examined and improved wind-forcing models with the aid of laboratory experiments in a wind-wave tank facility at the Korea Advanced Institute of Technology, Korea (with additional financial support from the National Research Foundation of Korea).

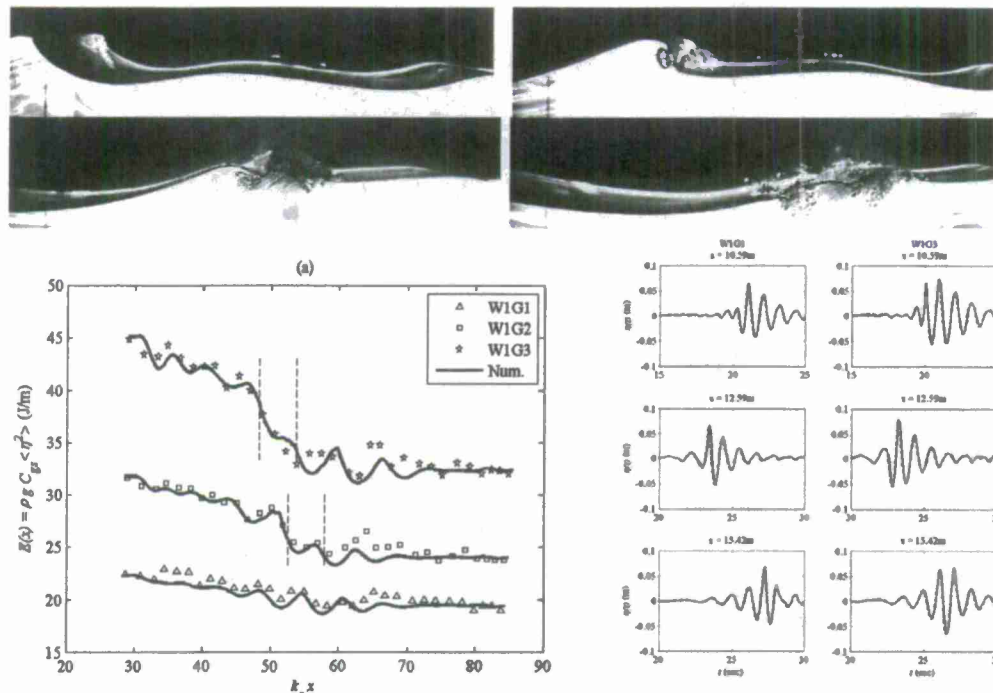


Figure 2.10. Top panel: Two-dimensional wave breaking in a wave tank at the University of Michigan. Bottom left panel: Comparison of the total energy as a function of space: symbols represent experimental measurements and solid lines represent numerical results. The vertical dash lines indicate the wave breaking region. Bottom right panel: Comparison of surface elevations measured from three wave stations. Solid line: experimental measurements; dash line: numerical results.

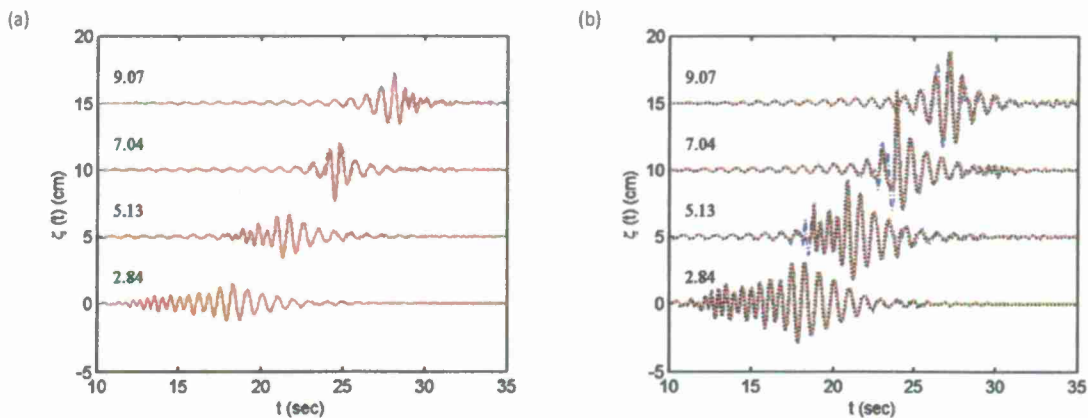


Figure 2.11. Surface elevation for the wave groups under wind condition $U_0 = 1.4$ m/s. (a) non-breaking wave group and (b) breaking wave group. Blue dash-dot lines: experiment; green solid lines: miles model; red dash lines: sheltering model; dark dot lines in (b): combination of the two models. Measurement locations downstream to the wavemaker are indicated in the figure, e.g. 2.84 m.

2.3.2 Radar Data Assimilation and Wave Forecasting

Personnel: Okey Nwogu, University of Michigan
Sina Aragh, University of Michigan

Over the course of the MURI project, we developed a novel approach to assimilate wave measurements from a Doppler marine radar and forecast the nonlinear evolution of the wavefield. The wave forecast model, VORTWAVE, solves the exact kinematic and dynamic free surface boundary conditions expressed as a set of evolution equations for the free surface elevation and tangential velocities instead of the traditional approach based on the velocity potential. A velocity-based boundary integral equation is used to solve the Poisson equation at every time step and close the system of equations. Use of a velocity-based formulation instead of a potential flow one allows the wave model to be applied to problem involving nonlinear wave interaction with vortical flows such as strongly sheared wind-generated currents.

A technique was also developed to accelerate the wave model computations by expanding the boundary integrals in a wave steepness parameter and using the fast Fourier transform (FFT) method to evaluate the leading order contributions to the boundary integrals. This reduces the number of operations at each time step from $O(N^2)$ to $O(N \log N)$ for the boundary integrals and $O[(NM)^2]$ to $O(N \log N)$ for the volume integrals, where N is the number of horizontal grid points and M is the number of vertical layers, making the model an order of magnitude faster than traditional boundary/volume integral methods.

VORTWAVE was used to investigate the occurrence of rogue waves on vertically-sheared current fields. The numerical simulations demonstrated that the mean flow vorticity can significantly affect the growth rate of extreme waves in narrow band sea states. The effect of wave breaking was incorporated into VORTWAVE by idealizing the whitecap region on the front face of spilling breaking waves as an infinitely thin vortical layer that exerts a pressure on the underlying irrotational wave field. Numerical simulations of the post-breaking evolution of wave groups were compared to data from laboratory experiments conducted at the Institute of Ocean Technology of the National Research Council of Canada. Sample model-data comparisons of the time histories of transient breaking waves are shown in Figure 2.12.

A variational data assimilation technique was also developed to assimilate surface elevation data from non-coherent radars or radial velocity data from coherent radars into VORTWAVE. The data assimilation scheme determines an "optimal" wave field that minimizes a cost function defined as the squared difference between the measured data and numerical model predictions over an assimilation interval. The gradient of the cost function is evaluated by propagating the adjoint wave model backwards with a forcing function that is proportional to the difference between the forward model predictions and radar observations. Figure 2.13(a) shows a sample application of the data assimilation scheme to synthetic data. Uncorrelated Gaussian noise was added to model predictions to serve as radar observations. The forward model equations were then integrated using the noisy wave field as initial condition with the adjoint model used to iteratively correct the initial condition. Figure 2.13(b) shows the optimal initial condition recovered at the end of the assimilation scheme. The data assimilation scheme, in essence, eliminates most of the non-physical modes (noise) that do not satisfy the governing water wave evolution equations.

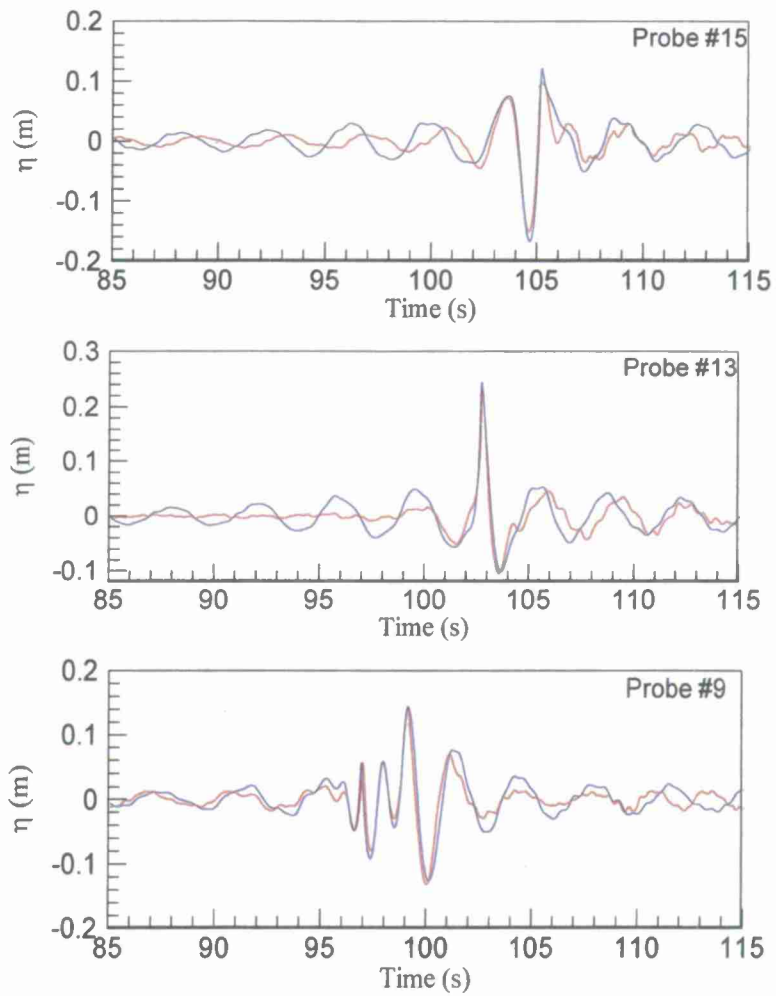


Figure 2.12. Measured and predicted time histories of transient breaking wave (red = measured, blue = num. model): pre-breaking (#9), breaking (#13) and post-breaking (#15)

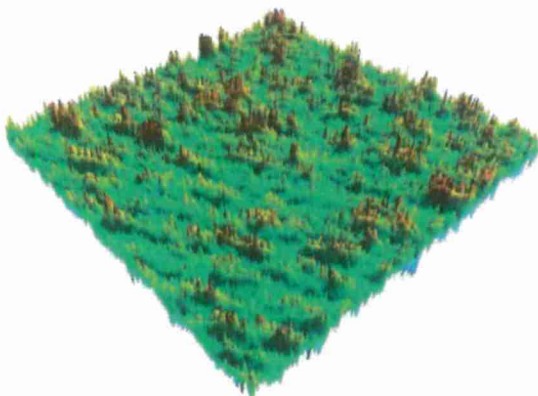


Figure 2.13(a) 3-D view of simulated initial condition with 50% noise.

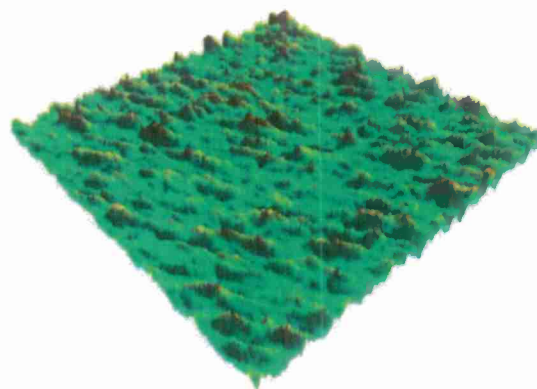


Figure 2.13(b) 3-D view of best-fit initial condition predicted by data assimilation scheme.

2.4 Ship Motion Prediction

2.4.1. Body-Exact Strip-Theory

Personnel: Robert F. Beck, University of Michigan
Xinshu Zhang, University of Michigan
Piotr Bandyk, University of Michigan
Rahul Subramanian, University of Michigan

The objective of this task was to develop a blended-method, time-domain seakeeping code that is computationally fast enough to use in real time path optimization. In typical blended-method codes the hydrostatic restoring forces, the incident wave (Froude-Krylov) exciting forces, and other external forces such as wind, propeller and rudder forces are computed in a nonlinear manner. Due to the large computational expense of three-dimensional nonlinear radiation and diffraction force calculations, linear or weakly nonlinear wave theories are often used in conjunction with strip theory to compute the radiation and diffraction forces.

We have developed a blended method that uses the nonlinear Euler equations of motion and integrates the hydrostatic and Froude-Krylov exciting pressures over the exact, instantaneous wetted surface. The dynamic wave pressure up to the exact free surface can be used directly if known or a Wheeler stretching can be used in conjunction with linear potential waves. The radiation and diffraction forces are found from body-exact computations. The body-exact computations are all done in the time domain. A fourth-order Adams-Bashforth method is used for the time stepping.

In body-exact computations, the Laplace equation is solved at each time step subject to a body boundary condition on the exact position of the body and linearized free surface conditions (both dynamic and kinematic) on the calm water level (i.e. $z=0.0$). The bottom boundary condition is automatically satisfied by the source distribution and the far field radiation conditions are met by using a beach along the outer boundaries. Desingularized sources are used above the free surface and flat panels with constant source strength are used on the body surface. Because the body-exact strip theory code is 10 times faster than the three-dimensional code, we have focused on the development of the Body Exact Strip Theory, or UMBEST, code. For a limited set of test cases for conventional hulls, the strip theory and three-dimensional codes give approximately the same answers.

The UMBEST code was developed as part of the Ph.D. dissertation of Piotr Bandyk (2009). Approximately one year ago, Piotr started working for DRS on the development of the U.S. Navy's new nonlinear, time domain ship motion code TEMPEST. The radiation and diffraction forces in the level 3.0 version of TEMPEST will be computed by the body-exact strip theory method developed under support of this project.

In the final two years of this project, the body-exact strip theory approach has been extended to the maneuvering/seakeeping problem. Traditionally, the problem has been solved by using a two-time scale approach (cf. Baily (1998) or Fossen (1994, 2005)). The slow time scale is the maneuvering and the fast time scale is at the wave frequency of encounter. The hydrodynamic problem is solved in a hydrodynamic axis frame that is set up to translate with an "assumed constant forward speed". The assumed speed is found by averaging over several previous wave cycles. This approach has the advantage of being able to use a conventional stability derivative maneuvering model with possible slight modifications to the seakeeping model. There are two difficulties with the approach. First, the assumed forward speed is somewhat arbitrary in that the number of wave cycles over which to average is determined by the user. Secondly, many of the interactions between the hydrodynamic forces developed on the body due to the seakeeping and the maneuvering will be lost. In an ideal world, one would like to

solve the maneuvering and seakeeping problems together as a single large problem. Modern unsteady CFD computations certainly use this approach, but at the cost of extremely large computational times.

In order to develop a computationally fast seakeeping/maneuvering code, the approach we have taken is to build on the original body-exact strip theory and to modify the hydrodynamic axis. The hydrodynamic axis that we use follows the ship. The x-y plane is coincident with the calm water plane and the z-axis is positive upwards. The origin of the hydrodynamic axis is on a vertical line with the origin of the body axis. The projection of the body x-axis on the calm water plane is coincident with x-axis of the hydrodynamic axis. Consequently, relative to the inertial frame fixed in space, the hydrodynamic axis follows the path of the ship with the same longitudinal and lateral velocities and the same yaw rate. In this hydrodynamic frame the body-exact problem can be set up to find the hydrodynamic forces acting on the ship. Once the hydrodynamic forces are known, Euler's equations of motion can be solve in the body fixed frame in order to determine the motions of the ship (both the maneuvering and seakeeping). There is no need to use an assumed average forward speed in the seakeeping computations, and, more importantly, the maneuvering and seakeeping problems have not been separated. All the viscous effects can still be brought in as needed based on the instantaneous velocities and accelerations of the body axis.

Sample results for maneuvering in waves are given in Figures 2.14 and 2.15; many more results for both the drifting problem and all 6-dof motions are available in Subramanian (2012). The results presented in figures 2.14 and 2.15 were simulated such that the hydrostatic and Froude-Krylov forces were integrated to the exact wetted surface but the radiation and diffraction problems were solved only up to the mean free surface. This is expedient for relatively low wave heights considered in the figures.

The ship chosen for the test case is the S175 containership because a great deal of experimental data is available. Extensive convergence studies have been conducted. For the results in figures 2.14 and 2.15, 60 panels were used on the complete midship section, with appropriate reductions in the number of panels on the bow and stern stations. There were 25 nodes per wavelength on the free surface, with the lateral extent of the computational domain being 4 wavelengths on each side. A two-wavelength long beach was used on each side to cancel out the far field waves. The time step size was the wave period divided by 200. The program presently is using the rudder, propeller and calm water resistance models of Son and Nomoto (1982). These are classic maneuvering model approaches with nondimensional coefficients based on model tests. Future research should involve developing improved models for the rudder, propulsion and resistance forces. In addition, the computations were done by dropping the mean forward speed times n_1 from the body boundary condition in the strip theory calculations. This term would give the wave resistance in a conventional 3-D panel method. In strip theory it is not valid. Furthermore, there would be a double count since the wave resistance is included in the empirically obtained calm water resistance force.

Figure 2.14 shows the predicted calm water turning circle for a Froude number of 0.15. Also shown are the free running model test experiments of Yasukawa and Nakayama (2009). As can be seen, the agreement is reasonable. Small changes in the modeling coefficients (particularly the rudder and propeller force models) would probably bring the results into line. Figure 2.15 presents the same results for running in beam seas at a Froude number of 0.15. The wavelength is $\lambda/L = 1.0$ and the wave height is a fairly steep $H/\lambda = 1/50$. The experimental and numerical turning circle results show the equivalent behavior; both drift down wave and to the right. The primary difference is the size of the turning circle. Again, changing Son and Nomoto model for the rudder and propeller would modify the turning circle. Also shown are the roll, pitch and heave motions as a function of time during the maneuver. The variable frequency of encounter is clearly seen and as is the changing amplitudes of the responses as the ship changes heading relative to the waves. In following seas (approximately $178 t/T$), the roll is small while the heave and pitch are much larger. In beam (approximately $190 t/T$) and quartering seas, the pitch becomes very small while the roll and heave are near their maximums.

References

- Baily, P.A., Price, W.G. and Temarel, P. (1998) "A unified mathematical model describing the maneuvering of a ship traveling in a seaway," *Transactions, RINA*, Vol. 140, 131-149
- Bandyk, P.J. (2009) "A body-exact strip theory approach to ship motions computations," Ph.D. dissertation, The University of Michigan, Department of Naval Architecture and Marine Engineering.
- Fossen, T.I. (1994) "The modeling of marine vehicles," in *Guidance and Control of Ocean Vehicles*, John Wiley and Sons, Chapter 2, pp 5-56
- Fossen, T.I. (2005) "A nonlinear unified state-space model for ship maneuvering and control in a seaway," *Journal of Bifurcation and Chaos*.
- Son, K. and Nomoto, K. (1981) "On the coupled motion of steering and rolling of a high speed container ship," *Journal of The Society of Naval Architects of Japan*, Vol.150 (1981), pp.232-244 (in Japanese).
- Yasukawa, H. and Nakayama, Y. (2009) "6-DOF motion simulations of a turning ship in regular waves," *International Conference on Marine Simulation and Ship Maneuverability*.
- Subramanian, R. (2012) "A time domain strip theory approach to predict maneuvering in a seaway," Ph.D. dissertation, The University of Michigan, Department of Naval Architecture and Marine Engineering.

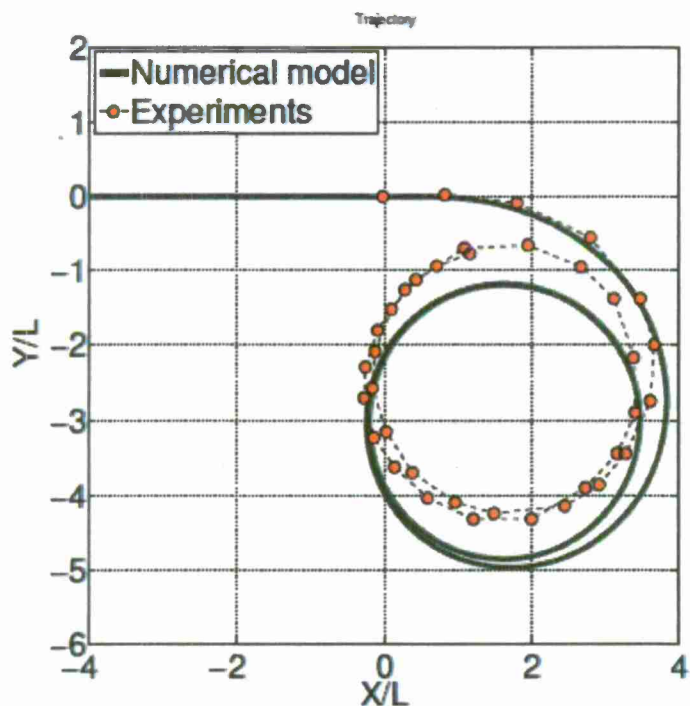
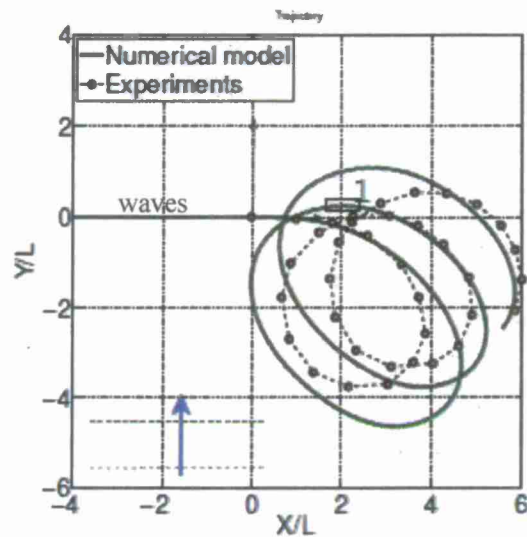
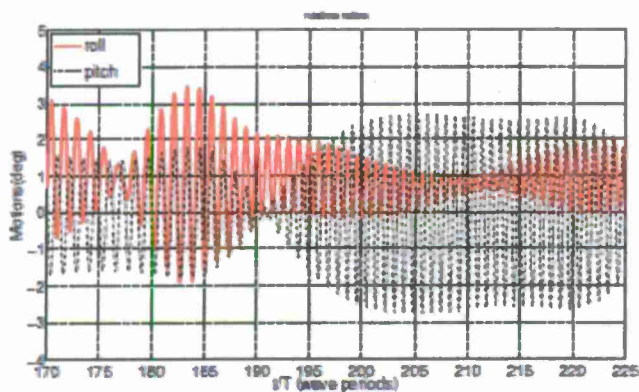


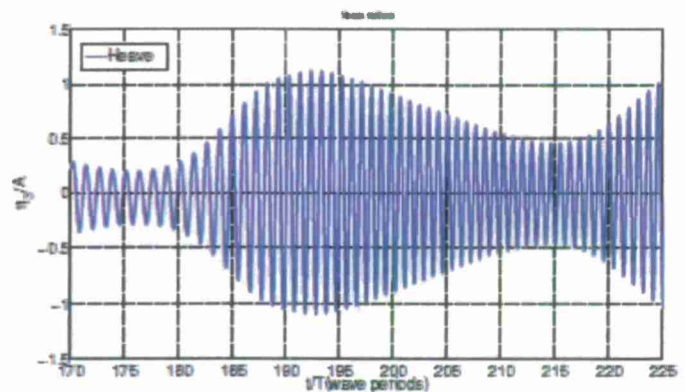
Figure 2.14. Calm water turning circle for S-175 container ship using Son and Nomoto (1981) models for the rudder, propeller and calm water resistance. $F_n = .15$, rudder angle = 35°



(a) Trajectory



(b) Details of roll and pitch motions



(c) Details of heave motions

Figure 2.15 S-175 turning circle and motion responses in beam seas.

Froude number = 0.15, rudder angle = -35° , regular waves with $\lambda/L = 1.0$, $H/\lambda = 1/50$.

2.4.2. 3-D Pseudo-Spectral Method

Personnel: Okey Nwogu, University of Michigan

Preliminary work was also started on extending the nonlinear pseudo-spectral wave model to predict the 6-dof motions of vessels moving along an arbitrary path in random multidirectional wavefields. The wave-body interaction problem was solved by: 1) time stepping the equations of motion for the free surface and body surface, and 2) solving the boundary value problem at every time step with a velocity-based boundary integral method. For surface-piercing bodies, the boundary-integral method is applied to both the physical fluid domain outside the body and a fictitious fluid region inside the body. The integrals over the free surface are then efficiently evaluated with FFTs while the integrals over the body surface are evaluated using the constant panel method. The pseudo-spectral wave-body model was evaluated with

linear wave diffraction by a circular cylinder and forced heave/surge motions of a hemisphere. Figure 2.16 shows a three-dimensional view of surface waves interaction with the cylinder for incident wave conditions with $ka = 1$ and $ka = 0.01$. The predicted pressure distribution around the perimeter of the cylinder at $kz = 0.25$ is compared to Havelock's analytical solution in Figure 2.17. Fairly good agreement is obtained with the analytical solution with errors of the order of 2%.

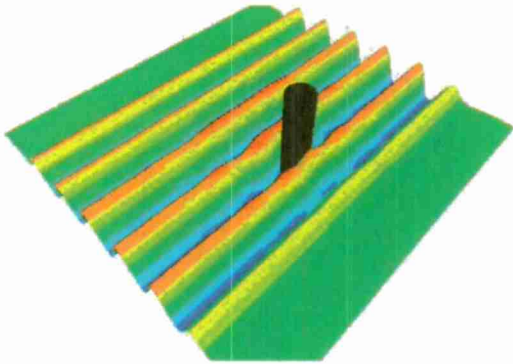


Figure 2.16. 3-D view of surface waves interacting with a cylinder, $ka = 1$.

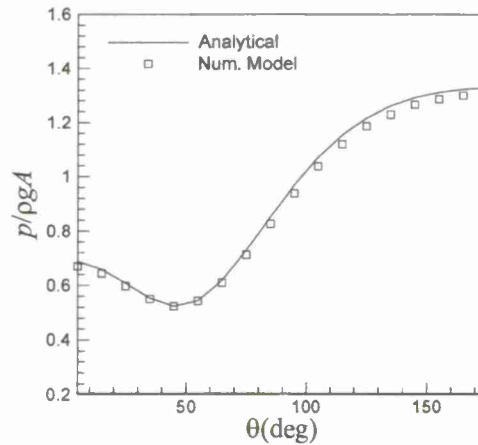


Figure 2.17. Comparison of predicted pressure distribution on cylinder surface with Havelock's analytical solution, $ka = 1$.

Predictions from FFT-accelerated 3D ship motion code have also been compared to results from the 2-D UM strip theory code for a slender vessel (Series 60, $C_B = 0.6$) in head seas at zero forward speed. As shown in Figure 2.18, good agreement was obtained between the two codes except for the shortest waves where diffraction effects become important and strip theory breaks down.

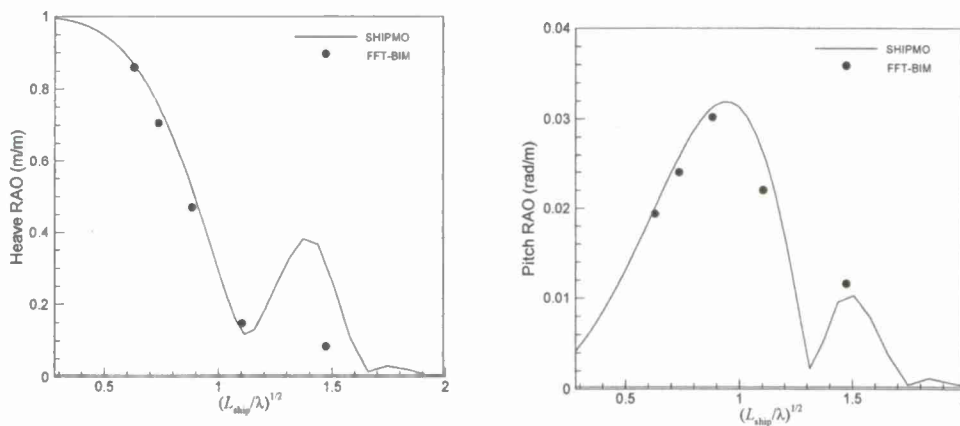


Figure 2.18. Comparison of the response amplitude operators for a Series 60 ($C_B = 0.6$) vessel in head seas ($U = 0$)

The 3D pseudo-spectral ship motion code was also applied to the MURI West Coast field experiments with the incident waves derived from the radar measured wavefield. The R/V Thompson ship hull was discretized with 240 panels as shown in Figure 2.19.

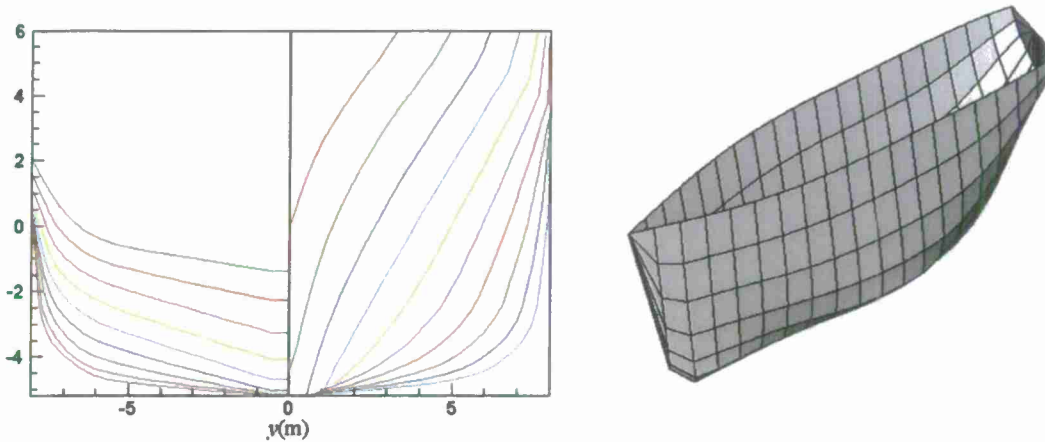


Figure 2.19. 3-D Panelization of R/V Thompson

Figure 2.20 shows a comparison of the measured horizontal (sway direction) and vertical motions at the ship motion sensor location on Aug 13, 2008 (17:00 GMT). Overall, the pseudo-spectral ship motion predictions are very similar to those obtained using the RAO-based ship motion code.

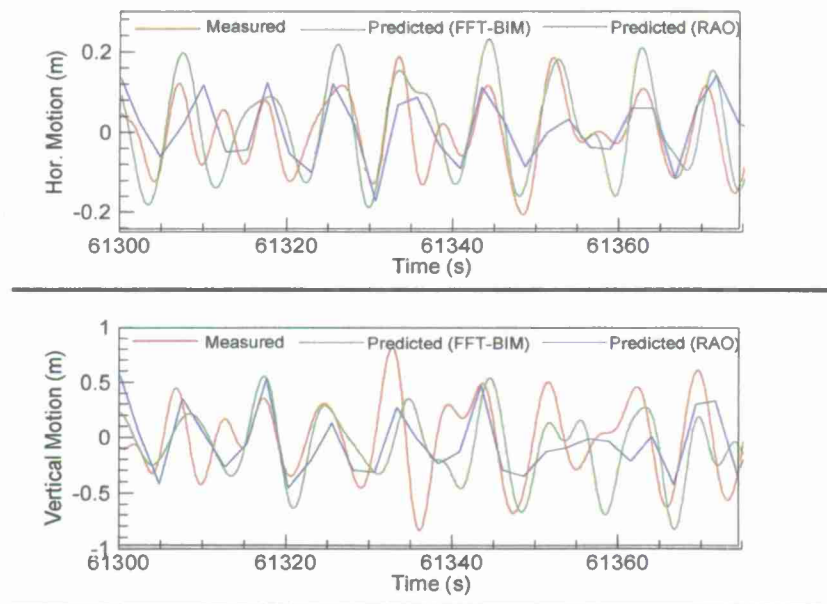


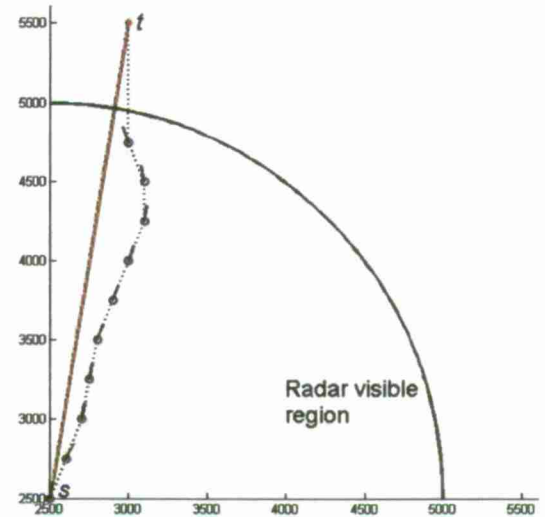
Figure 2.20. Comparison of measured R/V Thompson motions with predictions from the 3D panel and RAO methods [West Coast Field Experiments (Aug 13, 2008, 17:00 GMT)]

2.5 Real-Time Path Optimization and Vessel Control

2.5.1. Optimal Path Planning

Personnel: Robert L. Smith, University of Michigan
Irina S Dolinskaya, Northwestern University

The research goal of optimal path planning was to develop computationally efficient and numerically robust algorithms to solve ship path optimization problems in a time varying nonlinear wave-field. In the initial years' work under this grant, we found a closed form solution to a fastest path finding problem in a statistically stationary sea (time and space homogeneity); that is, where average vessel speed only depends on the traveling direction of the vessel in relation to the dominant wave direction. Next, we studied the general case with time and location dependence of the travel-time function. We developed a dynamic programming (DP) model that integrates the detailed wave-field information collected by the radar into the path planning process. We were able to integrate our earlier results for a stationary sea into the DP model in order to decrease the algorithm runtime, produce a smooth control-feasible fastest path, and incorporate the limitations of the radar visibility horizon. We developed MATLAB code that implemented our dynamic programming model and numerically tested the DP model in the simulated wave-field using the S-175 containership model. Based on our analysis, we observed up to 9.7% improvement in travel time and on average between 4% and 6% improvement over implementing the results for a stationary sea (neglecting radar collected data). When we scaled the minimum turning radius of the vessel by a factor of 0.5 (to simulate a more agile vessel) the improvements approximately double or tripled over the S-175 results. See figure for an example of the found fastest path (blue dashed line).



During the second half of the project, we focused on algorithms designed to find an optimal path that minimizes vessel root-mean-square (RMS) motion (roll) instead of travel time. Subsequently, we used the quasi-steady seakeeping and maneuvering model (MotionSim) developed by Drs. Robert Beck and Okey Nwogu's research group to numerically test the performance of our new algorithms. We developed a dynamic programming model that implicitly incorporates a trade-off between vessel roll and total travel time, as it is important to also consider the total travel time along a path in order to avoid extremely long detours with only marginal benefits to the motion objective function. The

Start												
xs	1270	1270	1270	1270	1270	1270	1270	1270	1270	1270	1270	1270
ys	1270	1270	1270	1270	1270	1270	1270	1270	1270	1270	1270	1270
heading	40	80	100	120	140	160	180	200	220	240	260	280
Target												
xt	2190	1480	1060	670	350	140	70	140	350	670	1060	1480
yt	2040	2450	2450	2310	2040	1680	1270	860	500	230	90	90
Optimal Path:												
TotalMotion	232.4	422.9	107.0	42.2	9.7	3.0	1.6	0.7	5.6	11.8	12.4	12.0
TotalNPoints	127	128	153	127	124	127	134	122	137	129	129	124
RMS Roll	1.35	1.82	0.84	0.58	0.28	0.15	0.11	0.07	0.20	0.30	0.31	0.31
Fastest Path (Line):												
TotalMotion	265.2	2053.5	640.9	72.0	10.7	4.7	2.9	0.7	10.2	48.2	31.2	20.0
NoPoints	121	121	121	122	121	122	122	122	121	122	121	121
RMS Roll	1.48	4.12	2.30	0.77	0.30	0.20	0.15	0.08	0.29	0.63	0.51	0.41
Roll Improvement	9%	127%	175%	33%	6%	29%	40%	6%	43%	108%	64%	30%
Travel Time Increase	5%	6%	26%	4%	2%	4%	10%	0%	13%	6%	7%	2%

numerical results in the table demonstrate that our procedure can lead to sizable reductions in RMS Roll for a modest increase in travel time. An example of optimal paths found by our algorithm, as well as the motions along the optimum path and the straight line path are presented in Figure 2.21.

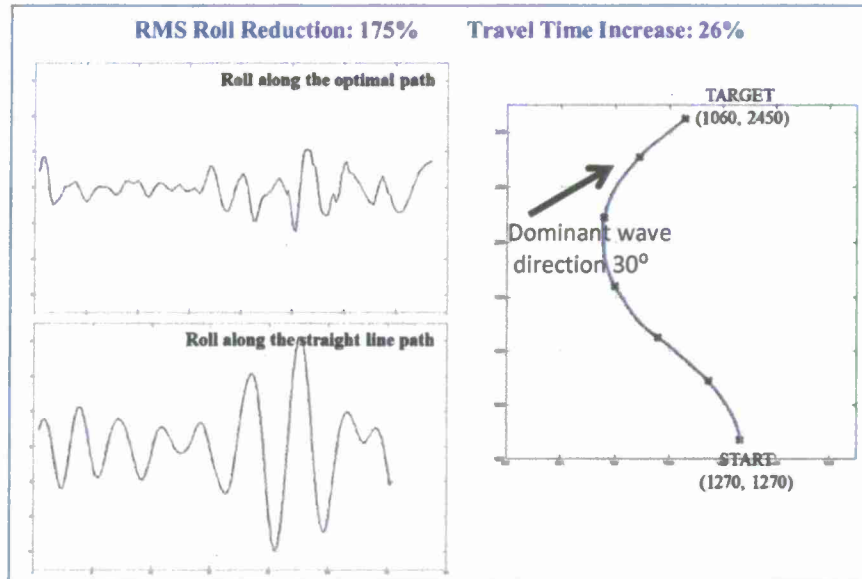


Figure 2.21. Roll reduction for optimal path following. S-175 in sea state 5 ($H_s = 3.25\text{m}$) and a ship speed of 10 m/s ($F_n = .24$) with a minimum turning radius of 300m. The RMS roll reduction along the optimal path was 175% and the additional travel time was 26%.

2.5.2. Adaptive Vessel Control

Personnel: Lingfeng Gao, University of Michigan
Jing Sun, University of Michigan

The objectives of this task are (1) to develop control strategies for vessel maneuvering in nonlinear wave fields with seakeeping constraints, (2) to investigate the robustness and stability properties of the integrated path-finding and path following control system, and (3) to develop effective numerical toolsets that can assist the design and performance evaluation of the vessel control system and can facilitate the total system integration. Over the course of the MURI project, we explored control methodologies and develop computational tools to address the path following problem with seakeeping constraints. In particular, we focused on the development of adaptive control schemes that can enhance system performance under varying operating environment and with model uncertainties.

The research efforts have led to 2 Ph.D dissertations, 7 journal and 9 conference publications. The main results and key contributions in the area of control and system integration areas are summarized as follows:

- *Control oriented model development:* A control-oriented 4 degree-of-freedom (surge, sway, yaw and roll) ship maneuvering model was developed and integrated with a wave model and a seakeeping model to represent the dynamic behavior of the ship in the nonlinear wave fields during the maneuver operation. The resulting model captures the first and second order wave effects on ship motion. The

model is developed in Matlab and has served as the major tool for control algorithm development, evaluation and validation.

- *Dynamic analysis and nonlinear control design for ship path following:* This effort resulted in a new notion of feedback dominance and a novel control design that uses the back-stepping procedure. Relying on feedback dominance, the resulting controller is almost linear, with very benign nonlinearities allowing for analysis and evaluation. Performance of the nonlinear controller, in terms of path following, is analyzed for robustness in the presence of rudder rate limits and saturation, as well as delays in the control execution. The simulation results reveal that the proposed controller enhances the path following capability, while demonstrating strong robustness against modeling uncertainties when applied to the nonlinear control model.
- *Development of the model predictive control for ship maneuvering with roll constraint:* Model predictive control (MPC) is explored to address the roll constraint for the ship maneuver operation. As the only available control approach that can explicitly handle hard constraints, MPC has a very flexible formulation that can be calibrated to fit most of the performance requirements but suffers from the computational complexity problem. Several mechanisms have been developed to reduce the computational burden of MPC, thereby making it more attractive for real-time control applications. Leveraging on those results, applications of MPC for ship path following satisfying roll constraints have been demonstrated (see Figure 2.22 for example). Moreover, the algorithm with improved computational efficiency allowed us to explore the coordinated rudder and propulsion control for path following.

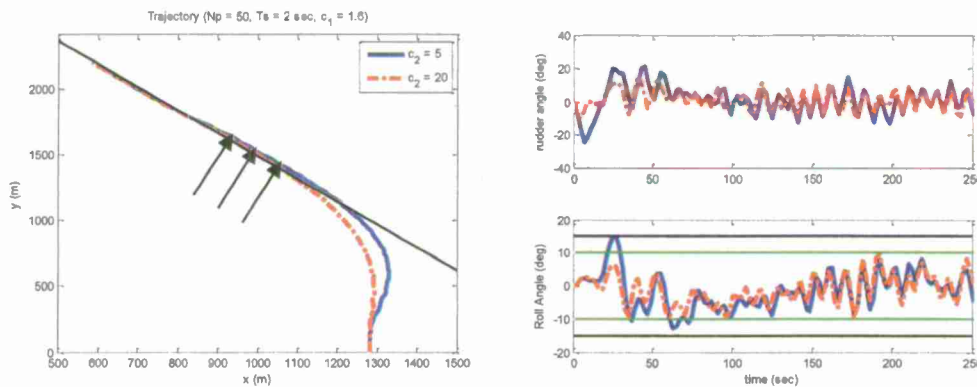


Figure 2.22. Simulation results of the ship response with the original (blue) and re-tuned (red) MPC path following controller in wave fields, green lines indicate the roll constraints.

- *Development of optimization-based control for path following and disturbance rejection:* A novel algorithm was developed that provides a mechanism to satisfy state constraints while achieving good system performance with low additional computational cost. The capability of this disturbance compensating MPC (DC-MPC) algorithm has been evaluated both analytically and numerically through an application to a vessel heading control problem and the results led to a full journal paper on the IEEE Transactions of Control System Technology.
- *Integration of path following control design with path planning:* The MPC was integrated with way-point path following to explore the trade-off between “staying on course” and “looking ahead”. Analytical investigation and numerical simulations have shown that, by incorporating optimal path planning, the proposed MPC way-point path following algorithm can achieve optimal way-point path following with moderate computational burden.

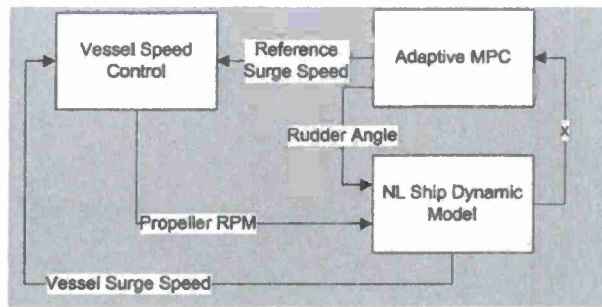


Figure 2.23. Adaptive MPC schematic for ship path following.

- Conceptualization and development of an adaptive model predictive control:* Adaptive MPC strategy was explored to address the path following problem with varying operating environment and model uncertainties. We leveraged the computational efficiency of the Parametric Neighboring Extremal (PNE) solution to develop an adaptive MPC algorithm for the ship path following problem, and addressed the real-time implementation and performance issues. The algorithm was applied to the ship path following problem to determine the optimal rudder angle and vessel surge speed, resulting in a control system shown in Figure 2.23. Implementation issues were identified and addressed; performance and computational efficiency were investigated and quantified.
- Development of a numerical test-bed with Matlab Virtual Reality Modeling Language (VRML):* The test-bed incorporates a control-oriented 4 degree-of-freedom (surge, sway, yaw and roll) ship maneuvering model, the model for the first order wave excitation force/moment, the model for the 2nd order drifting forces for the surge, sway, and yaw moment, and a wave disturbance model. Using Matlab Virtual Reality Modeling Language, the test-bed allows users to visualize the modeling and simulation results in an integrated environment. An example with the snapshot of the VRML model is shown in Figure 2.24, where the wave field, ship position, and path that the ship has followed are shown.



Figure 2.24. A snapshot of integrated numerical test-bed.

3.0 TECHNOLOGY TRANSITIONS

The accomplishments achieved under this project have been wide ranging and of importance to the Navy. The radar wave forecasting, nonlinear wave modeling and the ship motion research have all been directly transitioned over to the Navy FNC program entitled "Environmental and Ship Motion Forecasting (ESM F)." In addition, the computationally fast body-exact strip theory to predict the nonlinear responses of a ship to a seaway are being incorporated into version 3 of TEMPEST, the new, nonlinear, time-domain ship motion code that the Navy is developing.

4.0 PUBLICATIONS ACKNOWLEDGEING SUPPORT OF THE MURI

4.1 *Ph.D. Dissertations Supported by the MURI*

- Xinshu Zhang (2007) "Large-Amplitude Ship Motion Computations Using a Time Dependent Body Geometry," Univ. of Michigan
- Guangdong Pan (2008) "Electromagnetic Backscattering Studies of Nonlinear Ocean Surfaces." Ohio State University
- Piotr Bandyk (2009) "A Body-Exact Strip Theory Approach to Ship Motion Computations," Univ. of Michigan
- James Bretl (2009) "A Time Domain Model for Wave Induced Motions Coupled to Energy Extraction," Univ. of Michigan
- Irina Dolinskaya (2009) "Optimal Path Finding in Direction, Location and Time Dependent Environments," Univ. of Michigan
- Sina Hassanali-Aragh (2009) "Radar Data Assimilation and Forecasts of Evolving Nonlinear Wave Fields," Univ. of Michigan
- Zhen Li, (2009) "Path Following with Roll Constraints for Marine Surface Vessels in Waves Fields," Univ. of Michigan
- Kevin Zhigang Tian (2010) "A Study of Two-Dimensional Unsteady Breaking Waves in Finite Depth Water," Univ. of Michigan
- Matt Malej (2011) "Numerical and Asymptotic Modeling of Evolving Nonlinear Ocean Surface Wave Fields," New Jersey Inst. of Tech.
- Rahul Subramanian (2012) "A Time Domain Strip Theory Approach to Predict Maneuvering in a Seaway," Univ. of Michigan
- Chun-Sik Chae (2012) "Numerical studies of sea surface profile retrieval from low grazing angle scattering measurements," Ohio State University

4.2 *Book Chapters*

Dolinskaya, I.S. (2013). Dynamic Navigation in Direction-Dependent Environments. forthcoming in *Dynamic Network Modeling in Complex Transportation Systems* edited by S. Ukkusuri and K. Ozbay

4.3 Journal Articles

Aragh, S.H. and Nwogu, O. (2009). Variational assimilation of synthetic radar data into a pseudo-spectral wave model. *J. Coastal Research*, **52**, 235-244.

Bandyk, P. and Beck, R.F. (2011). The acceleration potential in fluid-body interaction problems. *Journal of Engineering Mathematics*, **70**, 147-163.

Chae, C.S. and Johnson, J.T. (2011) A study of interferometric phase statistics and accuracy for sea surface height retrievals from numerically simulated low grazing angle backscatter data. *IEEE Trans. Geosc. Rem. Sens.*, *IEEE Trans. Geosc. Rem. Sens.*, **49**, 4580-4587.

Chae, C.S. and Johnson, J.T. (2012). A study of sea surface range resolved Doppler spectra using numerically simulated low grazing angle backscatter data," submitted to *IEEE Trans. Geosc. Rem. Sens.*

Choi, W. (2009). Nonlinear surface waves interacting with a linear shear current. *Mathematics and Computers in Simulation*, **80**, 29-36.

Choi, W., Goullet, A. and Jo, T.-C. (2011). An iterative method to solve a regularized model for strongly nonlinear long internal waves. *J. Comp. Phys.*, **230**, 2021-2030.

Johnson, J.T., Burkholder, R.J., Toporkov, J.V., Lyzenga, D.R. and Plant, W.J. (2009). A numerical study of the retrieval of sea surface height profiles from low grazing angle radar data *IEEE TGRS*, **47** (6), 1641-1650, doi:10.1109/TGRS.2008.2006833.

Dolinskaya, I. S., Kotinis, M., Parsons, M. G., and Smith, R. L. (2009). Optimal short-range routing of vessels in a seaway. *Journal of Ship Research*, **53**(3), 121-129.

Dolinskaya, I.S. (2012). Optimal path finding in direction, location, and time dependent environments," *Naval Research Logistics*, **59** (5), 325-339.

Dolinskaya, I. S. and Maggiar, A. (2012). Time-Optimal Trajectories with Bounded Curvature in Anisotropic Media. *International Journal of Robotics Research*, 31(14), 1761-1793.

Dolinskaya, I. S. and Smith, R.L. (2013). Fastest-path planning for direction-dependent speed functions. Accepted for publication *Journal of Optimization Theory and Applications*.

Ghaemi, R., Sun, J., Kolmanovsky, I. (2012). Robust control of constrained linear systems with bounded disturbances. *IEEE Transactions on Automatic Control*, **57** (10), 2683-2688.

Ghaemi, R., Kolamnovsky, I., and Sun, J. (2011). Robust control of linear systems with disturbances bounded in state dependent set. *IEEE Transactions on Automatic Control*, **56**(7), 1740-1745.

Kent, C. and Choi, W. (2007). An explicit formulation for nonlinear waves interacting with a submerged body, *International J. Numerical Methods in Fluids*, **55**, 1019-1038.

Li, Z. and Sun, J. (2012). Disturbance compensating model predictive control with an application to ship heading control. *IEEE Transactions on Control System Technology*, **20**(1), 257-265.

Li, Z., Sun, J. and Beck, R.F. (2010). Evaluation and modification of a robust path following controller for marine surface vessels in wave fields. *Journal of Ship Research*, 54(2), 141-147.

Li, Z., Sun, J. and Oh, S. (2009). Design, analysis and experimental validation of a robust nonlinear path following controller for marine surface vessels. *Automatica*, **45**(7), 1649-1658.

- Nwogu, O. (2009). Interaction of finite-amplitude waves with vertically-sheared current fields. *J. Fluid Mechanics*, **627**, 179-213.
- Nwogu, O.G. and Lyzenga, D.R. (2010). Surface-wavefield estimation from coherent marine radars. *Geoscience and Remote Sensing Letters*, **7**, DOI:10.1109/LGRS.2010.2043712.
- Oh, S., Sun, J., Li, Z., Celkis, E.A. and Parsons, D. (2010). System identification of a model ship using a mechatronic system. *IEEE Transactions on Mechatronics*, **15**(2), 316-320.
- Oh, S. and Sun, J. (2010). Path following of underactuated marine surface vessels using line-of-sight based model predictive control. *Ocean Engineering*, **37**(23), 289-295.
- Pan, G. and Johnson, J.T. (2006). A numerical study of the modulation of short sea waves by longer waves. *IEEE Trans. Geosc. Rem. Sens.*, **44**, 2880-2889.
- Pan, G. and Johnson, J.T. (2008). A numerical method for studying modulation effects in radar observations of the sea surface. *IEEE Trans. Geosc. Rem. Sens.*, **46**, 3632—3636.
- Perlin, M. Choi, W. and Tian, Z. (2013). Breaking waves in deep and intermediate waters. *Ann. Rev. Fluid Mech.*, **45** (available online).
- Plant, W.J. and G. Farquharson, G. (2012). Origins of features in wavenumber-frequency spectra of space-time images of the ocean, *J. Geophys. Res.*, **117**, C06015, DOI:10.1029/2012JC007986.
- Plant, W.J. and Farquharson, G. (2012). Wave shadowing and modulation of microwave backscatter from the ocean. *J. Geophys. Res.*, **117**, C08010, DOI:10.1029/2012JC007912.
- Plant, W.J. (2012). Whitecaps in deep water. *Geophys. Res. Ltrs.*, **39**, L16601, DOI:10.1029/2012GL052732.
- Tian, Z., Perlin, M. and Choi, W. (2008). Evaluation of a deep-water wave breaking criterion, *Phys. of Fluids*, **20**, 066604.
- Tian, Z., Perlin, M. and Choi, W. (2010). Energy dissipation in two-dimensional unsteady plunging breakers and an eddy viscosity model. *J. Fluid Mech.*, **655**, 217-257.
- Tian, Z., Perlin, M. and Choi (2011). W. Frequency spectra evolution of two-dimensional focusing wave groups in finite depth water. *J. of Fluid Mech.*, **688**, 169-194.
- Tian, Z. and Choi, W. (2012). Evolution of deep-water waves under wind forcing and wave breaking effects: Numerical simulations and experimental assessment, submitted to *Eur. J. Mech./B Fluids*.
- Tian, Z., Perlin, M. and Choi, W. (2012). An eddy viscosity model for two-dimensional breaking waves and its validation with laboratory experiments, *Phys. of Fluids*, **24**, 036601.
- Zhang, X and Beck, R.F. (2007). Computations for large-amplitude two-dimensional body motions. *Journal of Engineering Mathematics*, **58**, 177-189.
- Zhang, X, and Beck, R.F. (2008). Three-dimensional large amplitude body motions in waves. *Journal of Offshore Mechanics and Arctic Engineering*, **130**, 1-10.

Zhang, X., Bandyk, P. and Beck, R.F. (2010) "Time-Domain Simulations of Radiation and Diffraction Forces," *Journal of Ship Research*, Vol 54, No 2, pp 79-94

Zhang, X., Bandyk, P. and Beck, R.F. (2010) "Seakeeping computations using double-body basis flows," *Applied Ocean Research*, **32**, 471-482.

4.4 Conferences Papers

Aragh, S. and Nwogu, O. and Lyzenga, D.L. (2008). Improved estimation of ocean wave fields from marine radars using data assimilation techniques. *Proc. 18th Int. Offshore and Polar Eng. Conference (ISOPE)*, Vancouver, Canada, **3**, 565-572.

Aragh, S. H. and Nwogu, O. (2007). Variational assimilation of synthetic radar data into a pseudo-spectral wave model. *Proc. 9th Int. Symp. on Fluid Control, Measurement, and Visualization (FLUCOME 2007)*, Tallahassee, FL.

Bandyk, P. and Beck, R.F. (2008). Nonlinear ship motions in the time domain," *Proceedings 27th International Conference on Offshore Mechanics and Arctic Engineering*, Estoril, Portugal.

Bandyk, P. and Beck, R.F. (2009). Nonlinear ship motion computations using a time-domain body-exact slender-body approach," *Proceedings 28th International Conference on Offshore Mechanics and Arctic Engineering*, Honolulu, Hawaii.

Bandyk, P., Beck, R.F. and Zhang, X. (2010). Applications of the Ogilvie-Tuck Formulae to Ship Hydrodynamics. *Proceedings 29th International Conference on Offshore Mechanics and Arctic Engineering*, Shanghai, China.

Belknap, W., Bassler, C., Hughes, M., Bandyk, P.J., Maki, K.J., Kim, D.H., Beck, R.F. and Troesch, A. (2010) "Comparisons of body-exact force computations in large amplitude motion," *Proceedings 28th Symposium on Naval Hydrodynamics*, Pasadena, California.

Choi, W. and Lyzenga, D. R. (2006). Nonlinear surface wave dynamics in slowly varying ocean environments, *Proceedings of the 26th Symposium on Naval Hydrodynamics*, Rome, Italy.

Choi, W. (2005). A formulation of nonlinear surface waves in water of variable depth, *Proceedings of Waves 2005*, Madrid, Spain.

Edmund, D.O., Maki, K.J., Beck, R.F. (2011) "An improved viscous/inviscid velocity decomposition method," *Proceedings 26th International Workshop on Water Waves and Floating Bodies*, Athens, Greece, 41-45.

Gao, L., Ghaemi, R. and Sun, J. (2011). Nonlinear adaptive model predictive control for ship path following using parametric neighboring extremal approach. *Proceedings 11th International Conference on Fast Sea Transportation, FAST 2011*, Honolulu, Hawaii.

Ghaemi, R. Sun, J. and Kolmanovsky, I. (2010) A neighboring extremal approach to nonlinear model predictive control," *Proceedings of the 8th IFAC Symposium on Nonlinear Control Systems (NOLCOS)*, Bologna.

Ghaemi, R., Kolmanovsky, I. and Sun, J. (2010). Robust control of linear systems with bounded state dependent additive disturbances. *Proceedings of the 48th IEEE Conference on Decision and Control*, Atlanta, GA.

- Ghaemi, R., Sun, J. and Kolmanovsky, I. (2009). Robust control of ship fin stabilizers subject to disturbances and constraints. *Proceedings of the 2009 American Control Conference*. St. Louis, MO.
- Ghaemi, R., Sun, J. and Kolmanovsky, I. (2008). Overcoming singularity and degeneracy in neighboring extremal solutions of discrete-time optimal control problem with mixed input-state constraints. *Proceedings of the IFAC'08 World Congress*, Seoul.
- Li, Z., Sun, J. and Oh, S. (2010). Handling roll constraints for path following of marine surface vessels using coordinated rudder and propulsion control. *Proceedings 2010 American Control Conference*, Baltimore, MD.
- Li, Z., Sun, J. and Oh, S. (2009). Path following for marine surface vessels with rudder and roll constraints: An MPC approach. *Proceedings 2009 American Control Conference*. St. Louis, MO.
- Li, Z., Sun, J. and Oh, S. (2007). A robust nonlinear control design for path following of an under-actuated marine surface vessel. *Proceedings 2007 IFAC Control Applications to Marine Systems (CAMS'07)*.
- Lyzenga, D., Nwogu, O., Trizna, D. and Hathaway, K. (2010). Ocean wave field measurements using X-band Doppler radars at low grazing angles, *Proc. IEEE International Geoscience and Remote Sensing Symposium*, Honolulu, Hawaii.
- Lyzenga, D. and Nwogu, O. (2010). Shipboard radar measurements of ocean waves for real-time prediction of nonlinear ship motions," *Proc. 28th Symposium on Naval Hydrodynamics*, Pasadena, California, 12-17.
- Maki, K.J., Bandyk, P.J., Beck, R.F. and Kim, S-E. (2010). Frequency dependence of large-amplitude horizontal-plane motion," *Proceedings 28th Symposium on Naval Hydrodynamics*, Pasadena, California.
- Nwogu, O. and Beck, R.F. (2010). Efficient computation of nonlinear wave interaction with surface-piercing bodies with an FFT-accelerated boundary integral method. *Proc. 28th Symposium on Naval Hydrodynamics*, Pasadena, California.
- Oh, S., Sun, J. and Li, Z. (2008). Path following control of underactuated marine vessels via dynamic surface control technique," *Proceedings ASME 1st Control Conference*.
- Pan, G. and Johnson, J.T. (2006). A numerical study of the modulation of short sea waves by longer waves. *Proceedings Int'l Geoscience and Remote Sensing Symposium*.
- Pan, G., Burkholder, R.J., Johnson, T.J., Toporkov, J.V. and Sletten, M.A. (2006). Studies of ocean surface profile retrieval from simulated LGA radar data. *Proceedings Int'l Geoscience and Remote Sensing Symposium*.
- Pan, G. and Johnson, J.T. (2007). A numerical study of modulation mechanisms in sea backscattering," *Proceedings North American Radio Science Meeting*.
- Plant, W.J. and Farquharson, G. (2012). Wave shadowing and modulation of microwave backscatter from the ocean. *Proceedings Boulder URSI Meeting*.
- Plant, W.J. and Farquharson, G. (2012). Origins of features in wavenumber-frequency spectra of space-time images of the ocean. *Proceedings AGU Ocean Sciences Meeting*.

- Plant, W.J. (2012). Measurement of winds, waves, and currents with a shipboard coherent radar, *Proceedings IGARSS 2012*
- Rosemurgy, W.J., Edmund, D.O., Maki, K.J., Beck, R.F. (2011). A method for resistance prediction in the design environment," *Proceedings 11th International Conference on Fast Sea Transportation, FAST 2011*, Honolulu, Hawaii.
- Rosemurgy, W.J., Maki, K.J., Beck, R.F. (2012). A velocity decomposition approach for steady free-surface flow," *Proceedings 29th Symposium on Naval Hydrodynamics*, Gothenburg, Sweden.
- Subramanian, Rahul, Beck, R.F. (2012). Development of a time domain strip theory approach for maneuvering in a seaway" *Proceedings 27th International Workshop on Water Waves and Floating Bodies*, Copenhagen, Denmark.
- Subramanian, Rahul, Beck, R.F. (2012) "Time Domain Simulation of a Ship Drifting in a Seaway" *Proceedings 31st International Conference on Offshore Mechanics and Arctic Engineering*, Rio de Janeiro, Brazil.
- Tian, Z., Perlin, M. and Choi, W. (2010). Evolution of nonlinear surface waves under the effects of wave breaking and wind forcing. *Proceedings 28th Symposium on Naval Hydrodynamics*, Pasadena, California.
- Tian, Z., Perlin, M. and Choi, W. (2010). Observation of air flow separation over steep water waves. *Proceedings 29th International Conference on Offshore Mechanics and Arctic Engineering*, Shanghai, China.
- Tian, Z., Perlin, M. and Choi, W. (2011). Refining an eddy viscosity model for two-dimensional breaking waves in deep water: experiments. *Proceedings 30th International Conference on Offshore Mechanics and Arctic Engineering*, Rotterdam, Netherlands.
- Zaman, M. H., Parsons, W., Nwogu, O., Choi, W., Baddour, R. E. and Mak, L. (2008). Generation and propagation of long crested finite-depth surface waves – comparison between the corresponding results from numerical models and a wave tank. *Proceedings 27th International Conference on Offshore Mechanics and Arctic Engineering*, Estoril, Portugal.
- Zhang, X, and Beck, R.F. (2006). 2-D body-exact computations in the time domain. *Proceedings 21st International Workshop on Water Waves and Floating Bodies*, Loughborough, United Kingdom.
- Zhang, X, and Beck, R.F. (2007). Three-dimensional large amplitude body motions in waves. *Proceedings 26th International Conference on Offshore Mechanics and Arctic Engineering*, San Diego, CA. Also published in the *Journal of Offshore Mechanics and Arctic Engineering* (2008)
- Zhang, X, Bandyk, P. and Beck, R.F. (2007). Large Amplitude Ship Motion Computations in the Time Domain. *Proceedings 9th International Conference on Numerical Ship Hydrodynamics*, Ann Arbor, Michigan, 788-799.

REPORT DOCUMENTATION PAGE*Form Approved*
OMB No. 0704-0188

Public reporting burden for this collection of information is estimated to average 1 hour per response, including the time for reviewing instructions, searching data sources, gathering and maintaining the data needed, and completing and reviewing the collection of information. Send comments regarding this burden estimate or any other aspect of this collection of information, including suggestions for reducing this burden to Washington Headquarters Service, Directorate for Information Operations and Reports, 1215 Jefferson Davis Highway, Suite 1204, Arlington, VA 22202-4302, and to the Office of Management and Budget, Paperwork Reduction Project (0704-0188) Washington, DC 20503.

PLEASE DO NOT RETURN YOUR FORM TO THE ABOVE ADDRESS.

1. REPORT DATE (DD-MM-YYYY) 30-11-2012		2. REPORT TYPE Final Report		3. DATES COVERED (From - To) 1 April 2005 to 31 August 2012	
4. TITLE AND SUBTITLE Optimum Vessel Performance in Evolving Nonlinear Wave Fields				5a. CONTRACT NUMBER	
				5b. GRANT NUMBER N00014-05-1-0537	
				5c. PROGRAM ELEMENT NUMBER	
6. AUTHOR(S) Robert F. Beck				5d. PROJECT NUMBER	
				5e. TASK NUMBER	
				5f. WORK UNIT NUMBER	
7. PERFORMING ORGANIZATION NAME(S) AND ADDRESS(ES) University of Michigan Dept. of Naval Arch. & Marine Engineering 2600 Draper Drive Ann Arbor, MI 48109-2145				8. PERFORMING ORGANIZATION REPORT NUMBER Dept. Naval Arch. & Marine Eng. Report 350	
9. SPONSORING/MONITORING AGENCY NAME(S) AND ADDRESS(ES) Office of Naval Research Dr. Patrick Purtell Code 331 875 N. Randolph St, Suite 1425 Arlington, VA 22203-1995				10. SPONSOR/MONITOR'S ACRONYM(S) ONR	
				11. SPONSORING/MONITORING AGENCY REPORT NUMBER	
12. DISTRIBUTION AVAILABILITY STATEMENT Distribution Unlimited					
13. SUPPLEMENTARY NOTES					
14. ABSTRACT This report summarizes the research conducted under the MURI entitled "Optimal Vessel Maneuvering in Evolving Nonlinear Wave Fields." A radar system was developed to measure the wave field around the ship. A nonlinear pseudo-spectral wave model that accounts for wave-wave interactions, wave-current interactions, wave breaking and wind-wave effects has been developed to forecast in time and space the evolving waves around the ship. The radar wave field predictions that initialize the wave field model are improved using assimilation techniques. Two techniques were developed to compute the responses of the ship to the predicted wave field: A body-exact strip theory and a FFT accelerated boundary element method. The optimal path through the wave field that minimizes ship motions and travel time is found using a new dynamic programming model. Various control algorithms were investigated to allow the ship to follow the optimum path.					
15. SUBJECT TERMS radar wave measurements, wave field evolution, ship motions, optimal path, ship maneuvering and control					
16. SECURITY CLASSIFICATION OF:			17. LIMITATION OF ABSTRACT UU	18. NUMBER OF PAGES 37	19a. NAME OF RESPONSIBLE PERSON Robert F. Beck
a. REPORT UU	b. ABSTRACT UU	c. THIS PAGE UU			19b. TELEPHONE NUMBER (Include area code) 734-764-0282